POLITECNICO DI TORINO
Repository ISTITUZIONALE

EMI Reduction via Spread Spectrum in DC/DC Converters: State of the Art, Optimization, and Tradeoffs

Original
EMI Reduction via Spread Spectrum in DC/DC Converters: State of the Art, Optimization, and Tradeoffs / Pareschi, Fabio; Rovatti, Riccardo; Setti, Gianluca. - In: IEEE ACCESS. - ISSN 2169-3536. - ELETTRONICO. - 3:(2015), pp. 2857-2874. [10.1109/ACCESS.2015.2512383]

Availability:
This version is available at: 11583/2696604 since: 2020-06-04T00:15:38Z

Publisher:
Institute of Electrical and Electronics Engineers Inc.

Published
DOI:10.1109/ACCESS.2015.2512383

Terms of use:

This article is made available under terms and conditions as specified in the corresponding bibliographic description in the repository

Publisher copyright
IEEE postprint/Author's Accepted Manuscript

©2015 IEEE. Personal use of this material is permitted. Permission from IEEE must be obtained for all other uses, in any current or future media, including reprinting/republishing this material for advertising or promotional purposes, creating new collecting works, for resale or lists, or reuse of any copyrighted component of this work in other works.

(Article begins on next page)

19 May 2024

Received December 8, 2015, accepted December 20, 2015, date of publication December 28, 2015,
date of current version January 5, 2016.

Digital Object Identifier 10.1109/ACCESS.2015.2512383

INVITED PAPER

EMI Reduction via Spread Spectrum in DC/DC Converters: State of the Art, Optimization, and Tradeoffs

FABIO PARESCHI[1,2], (Member, IEEE), RICCARDO ROVATTI[2,3], (Fellow, IEEE), AND GIANLUCA SETTI[1,2], (Fellow, IEEE)

[1]Department of Engineering, University of Ferrara, Ferrara 44122, Italy
[2]Advanced Research Center on Electronic Systems, University of Bologna, Bologna 40125, Italy
[3]Department of Electrical, Electronic, and Information Engineering, University of Bologna, Bologna 40136, Italy

Corresponding author: G. Setti (gianluca.setti@unife.it)

ABSTRACT Spread spectrum is a technique introduced for mitigating electromagnetic interference (EMI) problems in many class of circuits. In this paper, with particular emphasis on switching DC/DC converters, we consider the most common and most efficient known spreading techniques, looking for spreading parameters that ensure the highest EMI reduction and the lowest performance reduction in the circuit where the spreading is applied. The result is an interesting tradeoff not only between EMI reduction and performance drop, but also on the EMI reduction itself when considering different EMI victim models. The proposed analysis is supported by measurements on two switching DC/DC converters: 1) based on pulse-width modulation and 2) based on the resonant converter class.

INDEX TERMS DC/DC converters, electromagnetic compatibility (EMC), electromagnetic interference (EMI), spread-spectrum.

I. INTRODUCTION

With the term electromagnetic interference (EMI) we usually refer to any *unintentional* power transfer between a source (circuit/system) and a victim (circuit/system), either being radiated (i.e., propagated through space) or conducted (i.e., propagated through a grounding, power or signal conductor).

EMI has always been an issue in electrical devices. In the early years of (analog) electronics the main concern was the generation of disturbances in the victim. Analog TV systems, for example, have been developed with a 50 Hz or 60 Hz frame-rate in order to minimize the flickering effect due to interference coming from nearby 50/60 Hz AC devices.

With today (digital) electronics, EMI-related problems have received considerable attention, as proven by the presence of many international regulations [1], [2] aiming to impose/guarantee the electromagnetic compatibility (EMC) of any electronic device. According to these regulations, EMC is linked with: *i*) the ability to fit the power spectrum of any interfering signal radiated/conducted by a circuit/system under a prescribed mask; *ii*) the ability of a circuit/system to withstand incoming electromagnetic interference at a given level. In other words, any electronic equipment must not generate EMI above a tolerable level, and must be not susceptible to EMI if below a tolerable level. With respect to this, it is worth stressing that the role of EMI sources is not limited anymore to high power circuits and transmission power lines, but all (digital) circuits are characterized by a non-negligible switching activity with relevant EMI emissions. At the same time, digital logic is susceptible to interference, which can compromise signal integrity and even generate out-of-service conditions.

Classic and general purposes approaches for EMI reduction aim at reducing the coupling between source and victim with shielding [3] (for radiated emissions) or filtering [4], [5] (for conducted emissions). Nevertheless, in many situations these approaches cannot be employed, and ad-hoc solutions are required. For example, in many mixed-mode or system-on-a-chip circuits, the source and the victim circuits belong to the same integrated circuit [6]–[8]. In this case, layout strategies have been proposed to mitigate the EMI problem [9], [10]. More specific solutions are, however, related to the particular applications.

We here concentrate on the solution first proposed in early '90s [11], [12] and known as *dithering*, or *spread spectrum* clocking, which has attracted increasing attention since

2169-3536 © 2015 IEEE. Translations and content mining are permitted for academic research only.
Personal use is also permitted, but republication/redistribution requires IEEE permission.
See http://www.ieee.org/publications_standards/publications/rights/index.html for more information.

its proposal. This technique can be applied to any circuit showing a non-negligible switching activity, such as digital circuits and switching power converters.

In this paper, we focus on the application of spread spectrum techniques to switching power converters, which are particularly important since they are ubiquitously adopted thanks to their high efficiency. They found several applications as DC/DC converters in low-power portable devices [13], as AC motor inverters [14]–[16] and in power-factor control units [17]. Unfortunately, they are a preeminent source of EMI due to their high-power commutations that generate large amplitude interferences [18]. Even if these techniques find applications also in medium- and high-power converters [14]–[17] we concentrate on low-power ones (i.e., mW to few W), due to their ubiquitous adoption in today electronic systems.

Ad-hoc solutions for EMI reductions in this class of circuits include avoiding sharp transients by a proper snubbers design [19]–[22], or reducing the antenna factor with a clever routing of high-power lines [23], [24]. These solutions aim to reduce the actual EMI emitted power and are quite efficient in particular at high frequencies, while the effectiveness at low frequencies may be limited. Conversely, spread spectrum techniques aim to alter the shape of conducted/radiated interfering power spectrum, reducing the level of the peak components as required by international regulations [1], [2]. The main idea grounding this technique is the introduction of a controlled *jitter* in the timing signal controlling the converter to avoid the perfect periodic behavior of all waveforms in the circuit, thus spreading the power of their spectral components over a bandwidth which depends on the jitter characteristics. Interestingly, this EMI reduction approach can be considered as an additional and complementary methodology with respect to classical ones mentioned above.

In recent years spread spectrum techniques have been used in many applications, ranging from class D amplifiers [25]–[28] to microprocessor clock generators [29], [30], electronic ballasts [31], and LCD display panels [32]. It has been also adopted in some recent communication protocols like Serial ATA [33]–[39], Display Port [40] and PCI Express [41]. Many general-purposes commercial clock generators with spread-spectrum capabilities are also available on the market [42]–[45].

The applications of spread spectrum techniques in DC/DC switching converters is also a widely studied topic [46]–[52], and even in this case several commercial product are already available [53], [54].

In this paper we are interested in two aspects of the application of the spread spectrum techniques to DC/DC converters. The first one is the *optimization* of EMI reduction. Despite the fact that this topic appears trivial, EMI measured level strongly depends on the measurements setting [55]. Many works developed their optimization strategy based on the theoretically computed EMI power spectrum [46], [49], [50], [56]. Only in a few recent papers [55], [57]–[59] optimization according to the setting imposed by regulations [60]–[62] has been considered. In this paper we propose a few suggestions to optimize EMI reduction accordingly to the EMI victim circuit point of view.

The second aspect we are interested in is given by the *consequences of the spreading* accordingly to the source point of view. EMI reduction via spread spectrum is always achieved at the cost of performance reduction. For example, it is known that spread spectrum in switching DC/DC converters generates a small increment in the output voltage ripple [55], [63]. However, this and similar aspects have rarely been considered in a spread spectrum system design.

With this purpose in mind, we first present in Sec. II a survey on spreading techniques proposed for and applied to switching power converters. Then, in Sec. III we report some considerations on how to model the EMI victim circuit and whether international regulations fit this model or not. Hence, in Sec IV we try to identify which parameters ensure the optimal trade-off between effective EMI reduction and DC/DC converter performance degradation. Then, in Sec. V EMI measurements on two different DC/DC switching power circuits are provided to support our analysis: the first one is a pulse-width modulated (PWM) based boost converter (class-D), while the second one is a resonant converter (class-E). Finally, we draw the conclusion.

II. SPREADING TECHNIQUES: THE EMI SOURCE POINT OF VIEW

EMC regulations require that the interfering signal power spectrum fits below a predetermined mask, i.e., that its peak level does not exceed a given value [1], [2]. According to this point of view, any digital circuit or switching power converter is a potential EMI source, due to the *narrow-band* characteristic of the spectrum of their typical signals (including those responsible for EMI), for which energy is mainly located around a fundamental tone and its harmonics. Spreading techniques aim to increase the EMC of these circuits by lowering the power spectrum peak value of an interfering signal at the cost of adding additional spectrum components to it. This is achieved by introducing a controlled jitter in the reference timing signal (i.e., the clock), i.e., by changing the *instantaneous working frequency*. The result is a modification of all signals synchronous with the reference clock, altering their conducted/radiated power spectrum. In other words, these techniques aim to turn narrow-band interference into a (usually more tolerated) background EMI noise. This is sketched in Fig. 1.

Since their conception, spreading techniques have been criticized since, according to some contributions, they do not actually reduce disturbances in a potential victim, but simply transfer interfering energy in a different bandwidth. One of the aim of this contribution is to address this issue and clearly explain in which conditions spread spectrum techniques offer significant advantages in EMI reduction. To do so, we also report a summary of the spreading techniques proposed in the literature and, differently to what is typical in most contributions we develop our consideration

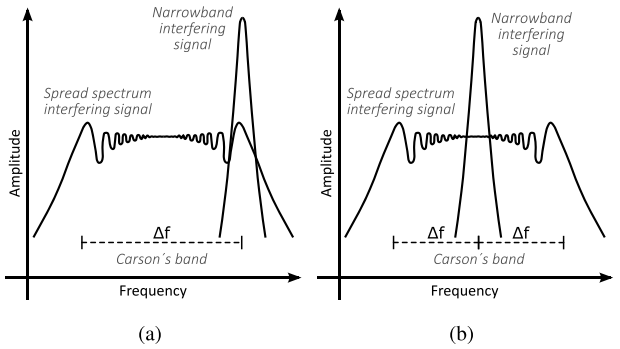

FIGURE 1. Sketch comparison between the power spectra of an unmodulated narrow-band interfering signal and of a spread spectrum one. (a): downspread; (b): center-spread.

not only with respect to EMI but also taking into account all the consequences of the introduction of spreading in the overall circuits/system behavior. As an example, reducing the time between two clock instants in a digital circuit reduces also the time available for computation. Since this has to be avoided, in almost all digital circuit only a *downspread* approach is allowed, i.e., the jitter can only increase the time between two clock instants. In other words, the instantaneous working frequency can only be reduced (see Fig. 1(a)). On the contrary, in switching DC/DC converters increasing the instantaneous working frequency is usually not an issue, and a centerspread approach as depicted in Fig. 1(b) is preferred.

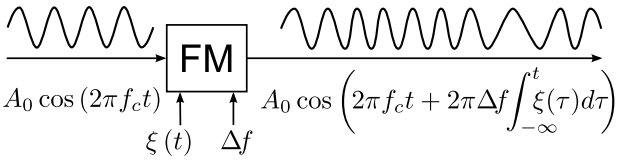

FIGURE 2. Classic approach for spreading a sinusoidal tone based on frequency modulation using a generic driving signal $\xi(t)$.

A. SPREADING BY FREQUENCY MODULATION OF TIMING SIGNALS

The most common way to achieve spread spectrum is by means of frequency modulation (FM) of the reference timing signal as schematized in Fig. 2. More formally, let us define $s(t)$ as the center-spread modulation of a simple sinusoidal tone

$$s(t) = A_0 \cos\left(2\pi f_c t + 2\pi\,\Delta f \int_{-\infty}^{t} \xi(\tau) d\tau\right) \qquad (1)$$

where f_c is the carrier frequency, Δf is the frequency deviation and $-1 \leq \xi(t) \leq 1$ is the (normalized) driving signal. The power of $s(t)$ is unchanged with respect to the unmodulated signal power and equal to ${A_0}^2/2$, and it is approximately spread [64] in the Carson's bandwidth $[f_c - \Delta f, f_c + \Delta f]$. Roughly speaking, in a frequency modulation of a sinusoidal tone we are changing the instantaneous signal frequency from $f_c - \Delta f$ (when $\xi(t) = -1$) to $f_c + \Delta f$ (when $\xi(t) = 1$) linearly with $\xi(t)$. When taking into account a more complex periodic signal (such as a clock or even the current waveform in a switching power converter inductor once steady state is achieved) applying FM is equivalent to apply (1) to each signal harmonic, with the only difference that the nth harmonic is spread within a bandwidth of amplitude $2n\Delta f$ [64].

Of course, the actual shape of the spectrum of $s(t)$ depends on the modulation parameters, i.e., Δf and $\xi(t)$. When $\xi(t)$ is a periodic function with period T, the spectrum of $s(t)$ is discrete, with components located at $f_c \pm k/T$, $k \in \mathbb{Z}$. Assuming a *fast* modulation, i.e., when T is short with respect to $1/\Delta f$ or, more precisely, when the *modulation index* $m = \Delta f \cdot T$ is small, only a few among these components[1] are significant in reducing EMI. Conversely, when we deal with a *slow* modulation, i.e., m is large, the (discrete) spectrum of $s(t)$ has many components very close the each other that can be assumed to be continuous in the Carson's bandwidth. This is the preferred situation for EMI reduction, since the shape of the spectrum is almost independent of the resolution of the measurement instrument.

It is worth stressing that a truly continuous power spectrum is obtained only with a non-periodic $\xi(t)$ such as that obtained using a true random generator. A pseudorandom-based generation of $\xi(t)$ is indeed a very good approximation, producing a the spectrum that, despite being actually discrete[2] presents components so close in frequency that would be almost impossible to distinguish between them in any practical measurement setting.

B. SHAPING THE SPECTRUM

How different $\xi(t)$ driving signals result in different $s(t)$ spectrum shape is sketched in Fig. 3 and can be described as follows.

The top plots correspond to the first spread spectrum system proposed by Lin *et al.* in 1994 [11] by modifying a simple, commercial PWM generator to achieve a sinusoidal modulation, i.e., $\xi(t)$ is a sinusoid. This approach is very simple from a circuital point of view, but also results in non-optimized performances in terms of EMI reduction, due to the presence of two peaks at both ends of Carson's bandwidth ($f_0 - \Delta f$ and $f_0 + \Delta f$). This is due to the fact that the power in the spectrum of the modulated signal concentrates at those frequencies corresponding to points of the modulating waveform where the time derivative is small, while it is reduced where the time derivative of the modulating waveform is large [65]. The effect, assuming a slow modulation, is an "u"-shaped continuous spectrum, similar to what depicted in the top-right plot of Fig. 3.

A better solution, proposed by Hardin *et al.* [12] exploits a *cubic* waveform $\xi(t)$, also known as

[1] Usually those in the Carson's bandwidth, which have a large enough amplitude and contribute to spread the energy of the original interference, thus reducing its spectrum peak.

[2] Pseudorandom sequences are periodic, even if with an extremely long period.

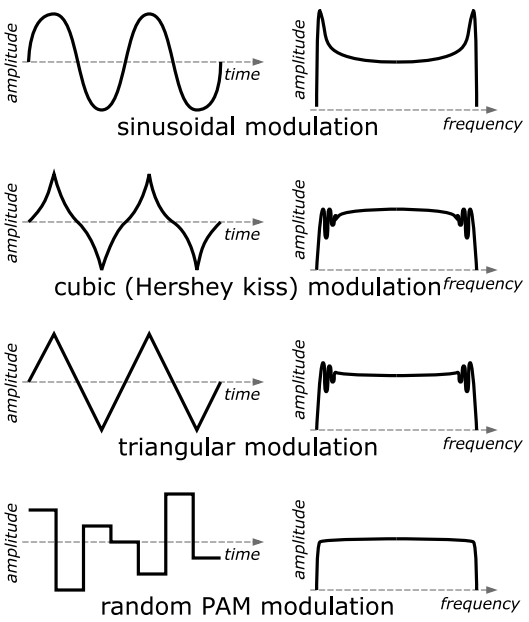

FIGURE 3. Sketch comparison between the output power spectra achieved with different $\xi(t)$ modulating signal. From top to bottom: sinusoidal modulation, cubic (Hershey kiss) modulation, triagular modulation, random PAM modulation.

Hershey-Kiss profile. The basic idea underlying this approach is to increase the time derivative of $\xi(t)$ around points corresponding to the peak values in the spectrum, and to decrease it where the power spectrum density level is low. As a consequence, $\xi(t)$ is a suitably distorted triangular waveform, whose time derivative is almost flat, with a small decrease around both ends of Carson's bandwidth to compensate peaks generated by some second-order effects. This solution ensures, under the assumption of a slow modulation (second plots from top in Fig. 3), a well-optimized EMI emission, and has been patented [30], used in some commercial devices [43], and considered in a few scientific literature works [66]–[68]. Nevertheless, its complexity is quite high, and a look-up table or a complex distortion circuit is commonly required to generate the required profile.

For the aforementioned reason, the most common approach in spread spectrum application is using a triangular $\xi(t)$ waveform. In other words, this approach ensures a flat time derivative profile, while small peaks generated by second-order effects around both ends of Carson's bandwidth (see third plots from top in Fig. 3) are tolerated and counterbalanced by the low complexity required to generate a waveform with a triangular profile (in particular in the digital domain, where an up/down counter is enough). This approach is in fact the most common one [29], [37], [69]. The main drawback, already mentioned by Hardin et al. in [12], is that if the triangular frequency is in the audible bandwidth, then an annoying whistle can be perceived during the circuit operation. For this reason, all commercial devices and standard protocols [30], [33], [40], [41] impose a triangular frequency immediately out of the audible bandwidth, and usually in the range 30-33 kHz. For a typical application, this value ensures a quite large modulation index m, justifying the continuous spectrum approximation of Fig. 3.

The solution corresponding to the bottom plots of Fig. 3 has been first proposed in [70] and then theoretically developed in detail in [56], and considers a pulse-amplitude modulated (PAM) spreading signal

$$\xi(t) = \sum_k x_k g(t - kT) \tag{2}$$

where $x_k \in [-1,\ 1] \subset \mathbb{R}$, $g(\cdot)$ is the normalized rectangular pulse $g(\tau) = 1,\ 0 < \tau < 1$ and 0 elsewhere, and T is the duration of the pulse. In order to distinguish between slow and fast modulations, we define a modulation index $m = \Delta f \cdot T$ exactly as in the previous cases.

In particular, results proposed in [56] are applied to a random PAM signal, i.e., where the $\{x_k\}$ sequence is randomly generated, and allow to get any desired spectrum shape under the two assumptions: *i*) a slow modulation is considered; and *ii*) we are able to generate $\{x_k\}$ with prescribed statistical properties. This approach has two main advantages:

- by employing a random sequence $\{x_k\}\ k = 0, 1, \ldots$, the resulting EMI spectrum is a continuous one, allowing a spectral shape that is actually independent of the measurement setting;
- the frequency $1/T$ is not constrained to be out of the audible bandwidth, since a random $\{x_k\}$ generate (white or colored) noise. This paves the way for additional optimization options [59].

Of course, in any practical circuit implementation, the required ideal random source can only be obtained with some approximation [71]–[73]. Several solutions have been proposed to this extent, each with different pros and cons. In [56] authors suggest to generate $\{x_k\}$ with a properly designed *chaotic map* [74], [75], i.e., an analog circuit implementing the update function $x_{k+1} = M(x_k)$, being M a suitable non-linear function $M : [-1,\ 1] \mapsto [-1,\ 1]$. The advantage of this approach is that it is relatively easy to shape the spectrum of the modulated timing signal (and of the interference) by suitably modifying M [75], [76].

Other approaches adopt a PAM $\xi(t)$, but prefer a simpler even if less versatile solution for the generation of the sequence $\{x_k\}$. A common solution [45], [77], [78] is to use a digital pseudo-random bit generator (PRBG), thus achieving a power spectrum which is discrete but close enough to a continuous one. In the commercial solution [45] a 9-bit PRBG and a 9-bit digital-to-analog converter (DAC) approximate a continuous $\{x_k\}$. A completely different solution can be found in recent works in the literature, which propose to use symbols x_k belonging to a restricted discrete set, and which is straightforwardly obtained by means of a simple finite-state machine. In [79] authors proposed a *binary* PAM modulation, i.e., $\{x_k\}$ is a random sequence where symbols can assume only the two values $x_k \in \{-1,\ 1\}$. Interestingly, this ensure the highest EMI reduction with respect to any known approach, but limited to the first harmonic only,

and constrained to a fast modulation with $m = 0.318$. Pareschi *et al.* [59] present a 16-level PAM, generated with a 4-bit finite-state machine implementing a permutation of the first 16 natural numbers, and converted into a $\xi(t)$ with a simple a 4-bit DAC. Even the limited number of level considered allowed to optimize EMI reduction in a realistic measurement setting.

C. OTHER SPREADING APPROACHES

Even if the modulation approach of Fig. 2 is the most commonly used, many other spreading techniques have been proposed in the literature.

Among them, it is worth mentioning the randomized PWM introduced, to the best of authors' knowledge, in [80]. Actually, different techniques are known with the terms ''randomized PWM''. All of them introduce a modification to the PWM waveform such as the period, the duty cycle D or the pulse delay, randomly changing it each time step. An overview of all these different approaches can be found in [81].

For example, in [82] a period modulation has been proposed, where the switching period of the DC/DC converter is randomly changed while the instantaneous duty-cycle is set by the PWM. In [51] and [52] authors propose to keep the switching period unchanged, and to randomly change the instantaneous value of D among a few fixed values. The random process selecting the instantaneous value of the duty cycle should impose an average D to set the output voltage to the desired level.

It is also known [83] that, when DC/DC converters are operating in hysteretic mode, i.e., when an external clock signal is not provided and the system is ''free-running,'', the converter can exhibit complex chaotic behavior. The effect is actually equivalent to consider a randomized PWM, and hysteretic control modes with chaotic behavior have sometimes been suggested as a way to reduce EMI [84], [85].

D. EFFECTS OF SPREADING TECHNIQUES ON EMI SOURCE CIRCUITS

As described in the previous sections, adopting spreading techniques has positive effects on the EMC of a circuit. In this section, we highlight other possible consequences in the circuit behavior. This is an important issue in practical applications, which is unfortunately often neglected in the literature.

For example, in any digital system (or digital communication system), changing the clock timing for spreading purposes means changing the time allowed for the elaboration or propagation of the signal. More precisely:

- as already mentioned, increasing the instantaneous frequency decreases the allowed time for elaboration/propagation. This is clearly in contrast with the design specification, and has to be avoided. For this reason, downspreading is mandatory in these applications;
- decreasing the instantaneous frequency increases the allowed time for elaboration/propagation. This is tolerated; however, there is a reduction in performance, since the computational power (or the throughput) is decreased.

In an asynchronous digital communication system an additional issue is related to clock recovery.[3] This is the case of the SATA computer bus interface, where perturbations in the transmitter clock result in an increased clock-to-data jitter at the receiver side. As such, timing perturbations introduced by spread spectrum clocking [34]–[39] must be in a limited, predetermined range imposed by the protocol standard in order to ensure a correct clock recovery [34], [39].

Another important case is related to switching power converters. As significant examples, we focus on two DC/DC circuits. The first one is the standard PWM based class-D boost topology shown in Fig. 4(a) [86], while the second one is the resonant class-E converter depicted in Fig. 4(b) and proposed in [87].

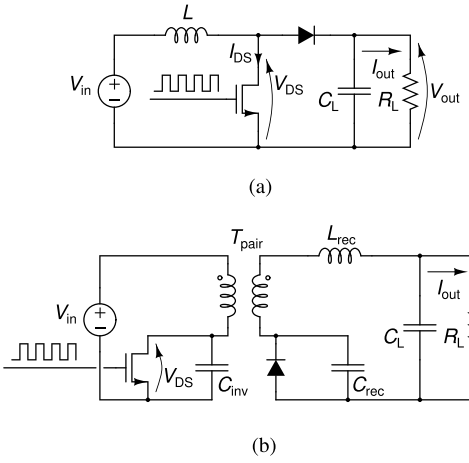

FIGURE 4. DC/DC switching converters considered in this paper. (a): PWM based class-D boost converter; (b): resonant class-E converter.

In the boost converter, the MOS switch is turned on and off with duty-cycle D at frequency f_c, generating an output voltage $V_{out} = V_{in}/(1 - D)$. The efficiency of the circuit is very high, since energy losses in the circuit are due only to non-idealities (e.g., the diode forward voltage drop, or the MOS transistor switching losses). The main issue is that the voltage waveforms across the MOS switch, the diode and the inductor have rectangular shape, with peak-peak amplitude approximately equal to V_{out} (V_{in} for the inductor), which turns the converter into a potential source of EMI. The converter EMC can be improved by exploiting spreading techniques on the signal driving the MOS switch, i.e., by changing the instantaneous working frequency f_c with respect to its nominal value. This however has a twofold consequence:

- on the output voltage ripple. The current across the diode has a rectangular waveform and it is filtered by the C_L-R_L low-pass filter to generate the ideally-constant output voltage V_{out}. Yet, a residual ripple is still present.

[3] In asynchronous communication the clock signal is, in fact, not transmitted and need to be recovered at the receiver side from the data stream.

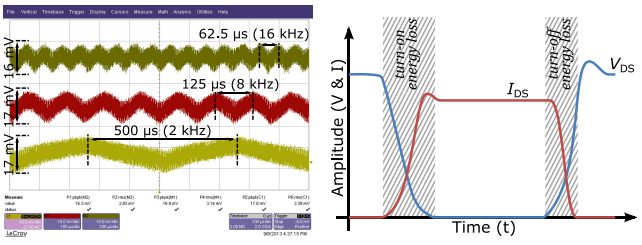

FIGURE 5. Effects of applying spreading techniques to PWM based DC/DC converters. (a): residual AM of the $\xi(t)$ on the output voltage observed in [55], increasing the ripple with respect to the standard (i.e., without spreading) case; (b): due to energy loss during turn-on and turn-off, the efficiency of the converter depends on its switching activity, that may be modified by applying spreading techniques.

The higher the working frequency, the greater the filtering effect, the lower the ripple. By introducing spreading, we have time intervals in which the instantaneous frequency is reduced and the ripple is slightly increased. A very few work in the literature [55], [63] have taken this problem into account. Fig. 5(a) is adapted from [55] and shows the output ripple of a buck DC/DC converter when a triangular spreading is applied for three different working periods $T = 500, 125, 62.5\mu s$. The figure shows a very limited dependence of the ripple value with $1/T$ and also highlights that a residual amplitude modulation (AM) of $\xi(t)$ is present on the output voltage.

- on the MOS transistor switching losses. These are mainly due to the limited turn on and turn off times of the MOS switch, i.e., every time we turn the MOS transistor on or off we have a short time period when $I_{DS}(t)$ and $V_{DS}(t)$ are simultaneously non-zero, as in Fig. 5(b), thus dissipating power. The total energy loss depends on the number of turn on and off events in a time period, i.e., it increases with the working frequency. The effect of applying spreading techniques on the total energy loss is a-priori unpredictable when using a center spreading approach, as the instantaneous frequency is sometimes increased, and sometimes decreased with respect to the nominal value. Furthermore, the presence of a (commonly adopted) feedback circuit with the aim of regulating the output voltage increases the unpredictability of the effects of spreading techniques on the efficiency. To the best of our knowledge, this effect has never been considered before in the literature.

In the case of the resonant class-E converter shown in Fig. 4(b) [87], the MOS switch is turned on and off at frequency f_c. However, this circuit exploits the so called *soft-switching* technique: the embedded resonant elements shape the drain/source voltage V_{DS} of the MOS switch in a sinusoidal-like way, synchronizing the zero-crossing instants of V_{DS} with the turn-on instant of the MOS transistor. This approach is known as zero-voltage switching (ZVS) and it is used to reduce the voltage-current product of the MOS at the switching instants, thus lowering (ideally, down to zero) the energy loss per cycle and allowing to increase the switching frequency of this converter topology up to the the very-high frequency (VHF) range (30-300 MHz) [88].

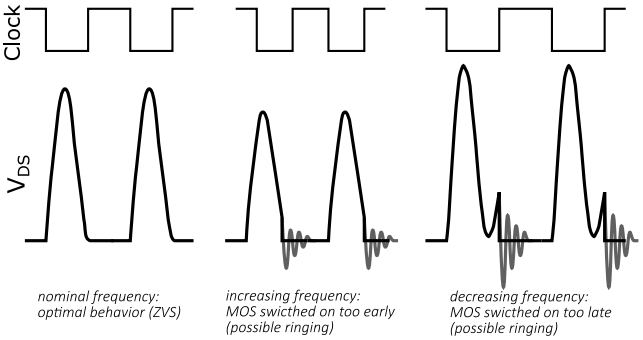

FIGURE 6. When oscillating at the nominal switching frequency f_c, the resonant converter features ZVS, i.e., the MOS is turned ON by its control clock signal when V_{DS} naturally reaches zero. When applying spreading techiques, the instantaneous frequency can be either be increased or decreased, and the MOS may be turned ON too early or too late. In this case, some ringing is possibly observed, and both behavior and emitted spectrum of the converter may be changed (figure adapted form [89]).

Note that only a very few works [89], [90] propose to apply spread spectrum techniques to resonant converters. The main reason is that here, differently from the PWM case, the working frequency f_c is a fundamental design parameter. For example, it is clear that the aforementioned ZVS condition is extremely sensitive to f_c. Fig. 6 is adapted from [89], and shows some chunks of the MOS switch drain/source voltage in a long SPICE simulation of the converter of Fig. 4b when a triangular modulation is applied. When the instantaneous switching frequency is equal to the nominal one f_c, the converter features ZVS, i.e., the MOS is turned ON when V_{DS} voltage naturally reaches zero. However, when applying spreading, the instantaneous switching frequency is continuously changed with $\xi(t)$, and ZVS may be not always ensured, since the MOS may be turned ON too early or too late. Even if a non-perfect ZVS is usually tolerated, we can observe that the V_{DS} waveform has a completely different shape in the three cases of Fig. 6. Furthermore, ZVS can be used to remove ringing effects in the V_{DS} waveform in real circuits. When ZVS is not ensured, ringing is commonly present, and this may alter both the converter behavior, and also the converter emitted EMI spectrum with respect to the expected one. In conclusion, the outcome of applying spreading must be considered with great care since it could not be limited to a reduction in converter performance.

III. SPREADING TECHNIQUES: THE EMI VICTIM POINT OF VIEW

Providing a general model for EMI victim circuits is not a trivial task. Many works in the literature presented a study on the EMI susceptibility of simple circuits such as a MOS differential pair [91], [92], a band-gap reference voltage [93], or a crystal oscillator [94]. For more complex or more general circuits several studies have presented experimental

radiation results [95], [96] or general guidelines for reducing EMI effects [97]. Interesting enough, other works present possibility to exploit high-power, high-frequency intentional EMI irradiation for generating denial of service attacks to electronic circuits [98]. However, also in this case, only experimental results are provided, without any theoretical background.

A. IS SPREAD-SPECTRUM EFFECTIVE OR JUST CHEATING?

Given the difficulty to define a precise general behavioral model of EMI victim circuits in presence of radiated or conducted interference, evaluating any EMI reduction strategy is not an easy task.

For this reason, immediately after its proposal in 1994, spread spectrum technique has been questioned, and accused to be a way for *cheating*, i.e., for passing international regulations without any actual advantage for the victim circuit. Many works have then been presented to support the spreading approach and to prove its effectiveness in reducing disturbances in practical situations, including TV signals decoding [99], on FM radio systems [100] and on wideband digital communications systems [101].

Nowadays, the effectiveness of spreading techniques is generally accepted, even if some questions are sometimes still raised. Accordingly to our experience, this is due mainly due to the difficulties in setting correctly the spreading parameters Δf and $\xi(t)$, and in the large differences that can be observed when EMI measurements are obtained with different settings.

With the aim of developing an unbiased discussion on the actual effect of spreading techniques, we think that is extremely important to focus on the following two questions:

1) how spreading parameters have to be set in order to reduce interference effects on a victim circuit?
2) which measurement settings allow good adherence between measurement results and interference effects on a victim circuit?

We will discuss the first question here and the second one later in Sec. III-B and III-C.

It is widely accepted that any EMI victim circuit can be modeled as lumped elements filters [95], [102]. This can be considered a straightforward assumption: it is, in fact, clear that, depending on the layout, on the topology, etc., a circuit is sensitive only to a few frequency ranges, and tolerant to other ones. The part of the spectrum of the EMI waveform falling in the (sensitivity) bandwidth of the filter produces an undesired output signal. This is superimposed to the desired output in an analog circuit, while the effect on a digital logic is to introduce, depending on its noise margin, a possible evaluation error.

The worst case scenario is when a large amount of power in the EMI signal spectrum is located at one of the victim sensitivity frequency ranges. In this case, a large noise signal will be generated, compromising the victim circuit signal integrity and increasing the probability of a victim failure. However, considering this only from a spectral (i.e., frequency domain) point of view is clearly not enough. If the interfering signal is non-stationary, the amount of power transferred to the victim may change over time. A frequency-domain-based analysis will take into account only the average power transferred to the victim, while the actual condition to be avoided is that the noise generated by EMI in the victim circuit is, at any time instant, below a critical level.

Accordingly to this observations, we propose a twofold approach in evaluating the optimal spreading parameters tuning, i.e., both from a frequency domain point of view and from a time domain point of view.

From the frequency domain point of view, since it is not possible to know a-priori the sensitivity bands of the EMI victim circuit, the best approach is to adopt a spreading approach whose spectrum is as flat as possible. International regulations requirements, by limiting the peak value of the interfering spectrum, are coherent with this point of view.

From the time domain point of view, we can recall that modulating a timing signal means changing its instantaneous frequency. There is a transfer of power between the EMI source and the EMI victim only when the instantaneous frequency of the interfering signal is exactly located in one of the victim sensitivity frequency ranges. In this case, the victim circuit behaves like a receiver filter tuned at the interfering signal frequency. However, like any linear or even non-linear filter, an (interfering) signal is generated in the victim only after a transient time: every filter has a settling time in which the output signal is initially very low, and only after a settling time reaches the steady-state value. This has been illustrated in Fig. 7. So, it is not relevant that the instantaneous interfering signal frequency enters or not into a victim sensitivity band, but it is mandatory that the time interval in which the instantaneous interfering signal frequency is within a victim sensitivity band is much shorter with respect to the settling time of the victim circuit. This is exactly the short-time effect discussed in [59].

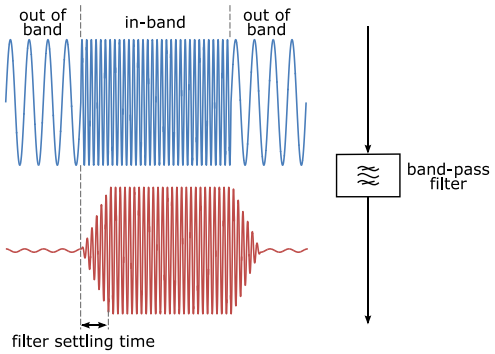

FIGURE 7. Example of settling time in a band-pass filter.

Of course, all the aforementioned observations stand under the assumption that the bandwidth in which the spectrum is spread by the adopted technique is much larger than the victim sensitivity frequency bandwidth.

Following these considerations, spreading is effective in reducing disturbances in a victim circuit if three conditions are satisfied:

- Δf is as large as possible;
- the interfering power spectrum is as flat as possible (which satisfy international regulations in an optimal way);
- a fast modulation is used, i.e. $\xi(t)$ is a fast varying signal.

Of course, the specific choice of Δf and the speed of variation of $\xi(t)$ over time will depend on the specific EMI victim circuit. However, based on our experience, ensuring the three above conditions grants significant reductions on the effects of EMI in the most general case.

The second open question is related to which measurement setup must be used to obtain results which are meaningful for evaluating the EMI effect on the victim circuit. To tackle this issue, in the next two sections we will consider the use of two different instruments: the dynamic signal analyzer (DSA) [103] and the analog spectrum analyzer, or EMI receiver [104].

B. THEORETICAL SPECTRUM: A NON-RELIABLE APPROACH

The most natural way to investigate spectral properties of a modulated signal is by means of its power spectrum [105]. Depending on the signal we are dealing with, different ways of computing the spectrum can be used. In the case of a FM of a simple sinusoidal tone as in Fig. 2, when $\xi(t)$ is periodic with period T, the spectrum is discrete, i.e., the signal can be decomposed in the sum of sinusoidal tones at frequency $f_c \pm k/T$, each one with amplitude A_k. The computation of the A_k for a sinusoidal modulation is known, and achieved with Bessel functions [11], while the case of the triangular modulation has been considered in [55]. When dealing with a random non-periodic $\xi(t)$, the achieved power spectrum is a continuous function, usually indicated with the terms power spectral density (PSD). In this case, the best solution to compute the PSD is to exploit the Wiener-Khinchin theorem, as in [56] which reports the PSD evaluation in the case of a PAM based random modulation.

Alternatively, the discrete Fourier transform (DFT) algorithm can help in estimating the theoretical spectrum of a signal either by means of numerical simulations or by the acquisition of a signal in a measurement session. The most common approach is using the DFT relying on the periodogram method, or exploiting its most commonly used modifications known as Bartlett's method and Welch's method. This approach is the spectral estimation method used by the DSA, and it is also embedded in many modern digital oscilloscopes [103].

Despite the fact that many papers rely on this approach, either from a theoretical/simulation analysis or from measurement with a DSA [46], [49], [50], [56], results achieved with this spectrum estimation method are not aligned with the considerations in Sec. III-A. This method, in fact, is not capable of taking into account the time domain aspects which are fundamental for a correct estimation of the EMI impact. To explain why, it is enough to consider the effect on the theoretical spectrum or on the one estimated by a DSA, when a triangular FM is considered for different values of m. The conclusion of [49] is that when m is increased, the number of spectral components in the Carson's band increases, so that the spectrum peak value is expected to always decrease. If one more correctly takes into account the effect of the finite frequency resolution R of a DSA,[4] the measured spectrum peak reduction reaches a saturation value for large m given by $10\log(R/(2\Delta f))$ [55]. The curves representing the peak value reduction in this situation, adapted from [55], are shown in Fig. 8 for different values of R taken as a fraction of Δf.

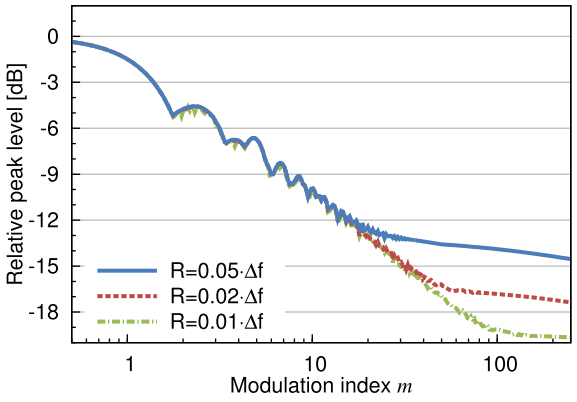

FIGURE 8. Relative peak level of the power spectrum of a triangular modulation (the 0 dB reference level is the unmodulated case) according to the theoretical power spectrum approach (either computed or measured with the periodogram method), assuming a finite resolution R. The EMI reduction increases with m, up to the saturation level $10\log(R/(2\Delta f))$ (figure adapted from [55], and achieved by setting Δf and changing T).

By looking at this figure, one would conclude that increasing m would always reduce the spectrum peak (until a saturation value) and would therefore be (almost) always beneficial in terms of EMI reduction. Unfortunately, such a conclusion would not be correct.

In fact, a larger value of m can be obtained by increasing Δf or T. A larger Δf has positive effects on the victim. Yet, by increasing T we are slowly changing the instantaneous interfering signal frequency, and the signal appears unmodulated for a long time. If this time is longer than the victim filter response time, we are not reducing at all the EMI effects on the victim circuit. For this reason, we do not consider the theoretical spectrum, as well as any approach based on this (including measurements taken with a DSA or a digital oscilloscope) as a reliable model for evaluating the effect of spreading techniques on a victim circuit.

C. EMI RECEIVER: A MORE RELIABLE APPROACH

International regulations require measurements to be taken with an EMI receiver [106], that is basically an analog spectrum analyzer with some additional input filters [104], [107]. Furthermore, regulations also set a prescribed setting

[4]This means that, when two spectral components are closer than R, they will appear as a single tone.

measurements method. For example, the resolution bandwidth (RBW) to be set in the instruments depends on the analyzed frequency band as indicated in Tab. 1.

TABLE 1. RBW and measurement type to be applied at different frequency ranges.

frquency range	RBW	measurement type
9 kHz-150 kHz	200 Hz	conducted
150 kHz - 30 MHz	9 kHz	conducted
30 MHz - 1 GHz	120 kHz	radiated
1 GHz - 18 GHz	1 MHz	radiated

There are practical and historical reasons for the choice of this instrument. In fact, up to a few years ago, it was the only one capable of measuring a spectrum in the GHz range. Furthermore, the RBWs to be set in the 150 kHz–30 MHz and 30 MHz–1 GHz correspond to the band reserved for a single channel in, respectively, the AM and FM radio broadcasting service, which were historically major sources of potential interferences.

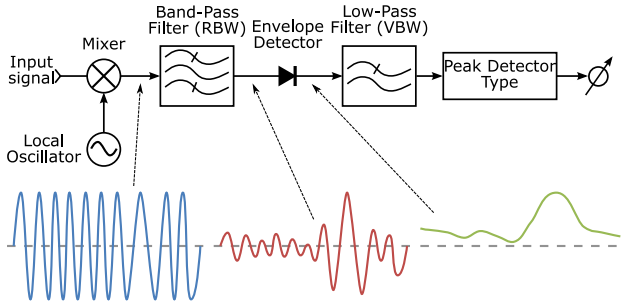

FIGURE 9. Simplified block diagram of an analog spread spectrum analyzer, including typical waveforms.

The basic working principle of the spectrum analyzer is that of the superheterodyne receiver of Fig. 9, along with some typical waveforms in order to better understand the behavior. The input signal is first mixed by a local oscillator, and then processed by the narrow band-pass RBW filter, whose bandwidth sets the instrument resolution. This solution is used to translate the frequencies of interest in the input signal into the RBW band, and it is a practical replacement for the ideal sweeping filter approach, where a tunable band-pass filter with bandwidth RBW is moved accordingly to the frequency range to be analyzed. The elements after the RBW filter are used to estimate the power of the filtered signal. More specifically, the signal is first demodulated and filtered by, respectively, the envelope detector diode and the low-pass video bandwidth (VBW) filter block (whose purpose is only to reduce noise on the instrument screen). Finally, the signal power is estimated using a suitable peak detector, that produces a single power value after observing the filtered and demodulated signal for all the measurement time. The local oscillator frequency is then moved to tune the RBW filter band on another frequency of interest.

Recently, time domain EMI receivers have been proposed [108], [109], with the aim of applying the aforementioned operations on a sampled version of the input signal. The advantage is to be able, with a massively parallel architecture, to analyze all frequencies in the range of interest at the same time, thus reducing measurement time that can be, with a standard EMI receiver, up to several hours [109].

Allowed standard choices for the peak detector are classically the *positive peak detector* and the *quasi-peak detector*, while recent instruments allows also the use of a few kinds of *average detectors* [104], [107]. The positive peak detector estimates the input signal power looking at the peak value of the demodulated signal during measurement time [104]. The quasi-peak and all average detectors achieve similar functions, though with a more complex behavior. In particular a few filtering stages with a controlled settling times are added to a standard positive peak detector [104], [110].

Note that the output of this architecture coincides with the theoretical spectrum only in simple stationary cases. However, by comparing the waveforms in Fig. 9 with that of Fig. 7, it is easy to conclude that the behavior of this instruments is very similar to that of the victim circuit in presence of EMI. Even if it is not possible to match the actual circuit sensitivity bandwidth and its settling time, the EMI receiver is a reliable model for EMI victim circuits. This is already a strong indication that any EMI optimization should be pursued using this instruments, and not by computing the theoretical spectrum.

Nevertheless, only a very few studies on spread spectrum techniques use an EMI receiver model [55], [57]–[59] to evaluate the spectrum of the interference. The main problem is the complexity and the non-linearity of the architecture in Fig. 9. The approach proposed in [55] is to study the system by using the standard analytical representation of a signal [105]. In this way, the non-linearity due to the envelope detector can be circumvented by considering only the modulus of the signal complex envelop. Conversely, the non-linearity due to the peak detector cannot be circumvented, and has to be numerically dealt with. With this approach, authors of [55] were able to develop optimization curves for EMI reduction via spreading techniques based on a triangular modulation. The curves for different values of RBW as a fraction of Δf (adapted from [55]) can be seen in Fig.10 and show that EMI reduction performance is decreasing when m increases after a certain value, as expected accordingly to the developed model for the EMI victim.

Note that the complexity of the architecture of Fig. 9 makes also quite difficult to numerically simulate the instrument behavior. The main issue is not the development of a simulator, and many of them have actually been proposed [108], [110]–[112].[5] The fundamental problem is, in fact, that simulating an EMI receiver is computationally a very heavy task.

To the best of authors' knowledge, all EMI receiver simulators can be divided into two main categories: one reproducing the behavior of the standard EMI receiver as in Fig. 9, and the other one reproducing a time domain EMI receiver.

[5]The Matlab simulator [112] is freely available from our website www.signalprocessing.it

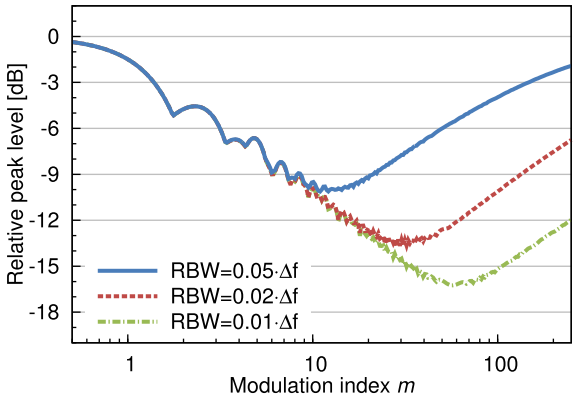

FIGURE 10. Peak level (the 0 dB reference level is the unmodulated case) of the triangular modulation power spectrum according to EMI receiver for different values of the ratio $RBW/\Delta f$ (figure adapted from [55] and achieved by setting Δf and changing T).

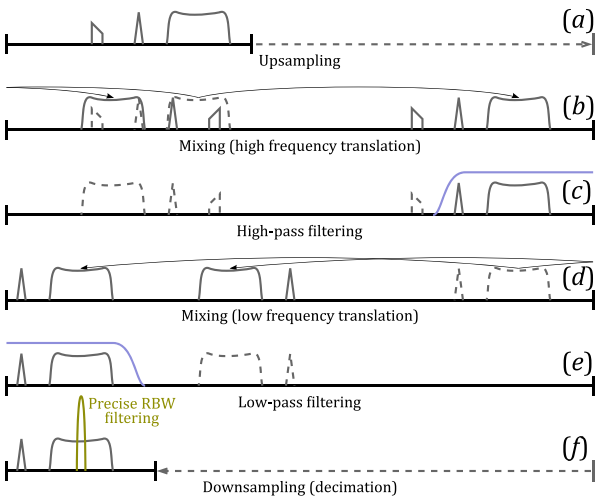

FIGURE 11. Frequency conversion steps in an analog spectrum analyzer. (*a*): upsampling; (*b*): frequency translation to upper frequency; (*c*): high-pass filtering to clean the spectrum at low frequencies; (*d*): frequency translation to low frequencies; (*e*): low-pass filtering; (*f*): decimation and application of a precise RBW filtering.

The simulator [112] belongs to the first category. It reproduces step by step the operations in an analog spectrum analyzer [104], including the several frequency translation and filtering steps illustrated in Fig. 11 which are required since every frequency translation obtained by mixing a signal with a sinusoidal tone generates two replica of the signal spectrum, one at higher and one at lower frequencies [103]. The input signal (being either locally generated or extracted from a transistor level circuital simulation) is first upsampled (Fig. 11 *a*), then a frequency translation to an upper frequency range is performed by mixing it with a sinusoidal tone, whose frequency is changed accordingly to the frequency range to be tuned into the RBW filter (Fig. 11 *b*). At this point, a digital implementation of the RBW filter could be applied; however, in order to avoid a computationally complex narrowband filtering at high-frequency, we adopt the same strategy as in real spectrum analyzer: the signal is filtered (Fig. 11 *c*) to clean the low part of the spectrum, and downshifted in frequency (Fig. 11 *d*), then filtered again (Fig. 11 *e*) in order to allow downsampling (Fig. 11 *f*) and a precise RBW filtering. After that, by means of a Hilbert transform, the signal envelope is extracted, filtered as in the VBW filter, and the peak detector is finally applied.

As in any other EMI receiver simulator, the most important issue is given by its complexity. The key concept is to keep the sampling frequency as low as possible in each step and, as the same time, avoid aliasing effects due to frequency replication. To this aim, it is fundamental to develop fast and effective decimation operations, that must include antialiasing filtering and can be conveniently divided into several steps.

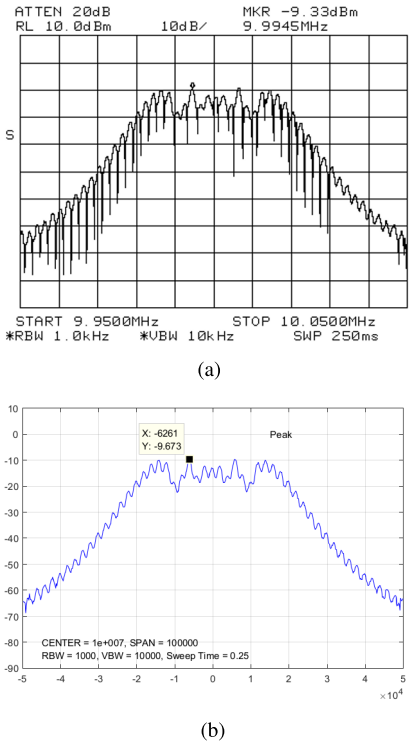

FIGURE 12. Comparison between the spectrum measured with an HP 8563E spectrum analyzer (a) and that achieved with the Matlab simulator (b), in a triangular based spreading modulation of a sinusoidal tone, with $f_c = 10$ MHz, $\Delta f = 20$ kHz and $m = 10$. In both cases the reference level (0 dB) has been set to the unmodulated sinusoidal tone.

This approach is very effective, as confirmed by the comparison of Fig. 12 between the spectrum achieved by the simulator and a measurement obtained from a HP 8563E analog spectrum analyzer, in the case of a triangular spreading of a sinusoidal tone with $f_c = 10$ MHz, $\Delta f = 20$ kHz and $m = 10$. Note that the Matlab simulation is extremely effective not only in identifying the shape of the spectrum, but also in computing the value of the peak (-9.3 dB for the measurement, and -9.6 dB for the simulation, both referring to an unmodulated sinusoidal tone).

IV. SPREADING SYSTEM OPTIMIZATION

On the basis of Sec. II and III, it is possible to develop some guidelines for setting parameters of timing signal spreading techniques to obtain the optimal trade-off between effective EMI reduction on the victim circuit and performance degradation on the source circuit. In particular, we consider three different modulation types on two different switching DC/DC converters. Measurements on these systems are provided in Sec. V.

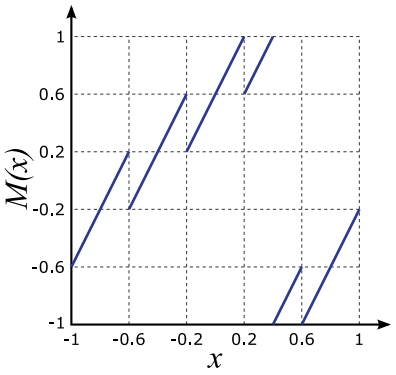

FIGURE 13. *M* function of the chaotic map considered in this paper, normalized into the interval [−1, 1].

The three considered spread spectrum approaches are achieved by FM of the reference timing signal as in Fig. 2. In particular they are:

- the standard triangular modulation;
- the PAM modulation using an $\{x_k\}$ sequences generated by the chaotic map proposed in [59] and depicted in Fig. 13. The particularity of the map in Fig. 13 is that it has been designed to generate optimal sequences for EMI reduction. More precisely, generated sequences satisfies the following two conditions

$$\begin{aligned} |x_{k+1} - x_k| &= |M(x_k) - x_k| \geq 0.4 \\ |x_{k+2} - x_k| &= |M(M(x_k)) - x_k| \geq 0.4 \end{aligned} \tag{3}$$

  which ensure a minimum distance between any couple of symbols with time-distance equal to one and two steps. In other words, this M ensures that the $\xi(t)$ is a fast enough varying function, as required in Sec. III;
- the PAM modulation using the 4-bit permutation based (pseudorandom) sequence proposed in [59]. The sequence is generated by the simple update function $z_{k+1} = z_k + 3 \pmod{16}$, and rescaled to get the sequence $\{x_k\}$ in the normalized interval $I = [-1, 1]$. All generated sequences satisfy

$$\begin{aligned} |x_{k+1} - x_k| &\geq 0.4 \\ |x_{k+2} - x_k| &\geq 0.4 \\ |x_{k+3} - x_k| &\geq 0.4 \\ |x_{k+4} - x_k| &\geq 0.4 \end{aligned} \tag{4}$$

  which is an even stronger condition with respect to (3), as it ensures a minimum distance between two symbols within four time steps. The $\xi(t)$ generated with this sequence is even faster varying with respect to that generating with the previously considered chaotic map.

A short time capture window, showing an example of the three driving functions $\xi(t)$, can be observed in Fig. 14.

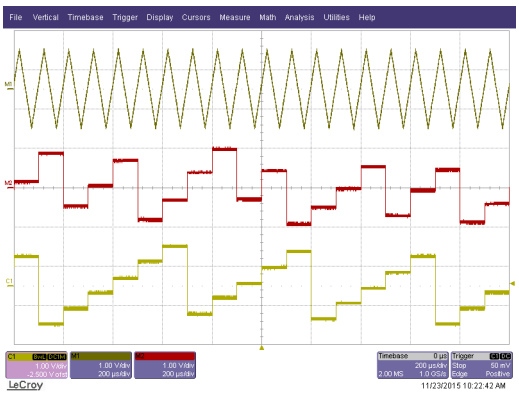

FIGURE 14. Different driving signals $\xi(t)$ considered in Sec. IV. From top to bottom: triangular waveform, chaotic map signal and permutation-based (pseudorandom) signal. All signals are in the same voltage range [−1, 1] V and generated with the same *T*.

These modulations are applied to two DC/DC switching converters. The first one is a LM3424 evaluation board [113] from Texas Instruments. This board embeds a PWM controller specifically designed for LED drivers, i.e., it has a constant output current (more precisely, 1 A output), a quite large voltage ripple (about 100 mV),[6] and it is designed in a boost configuration. The internal PWM controller can operate with adjustable switching frequencies of up to 2 MHz, and external synchronization is possible, allowing spread spectrum to be added by means of an external clock generator. The board has been loaded with a 22 Ω power resistor.

According to Sec. II, Δf should be small to limit the effects on the output ripple. Yet, according to Sec. III, Δf should be large to reduce interference on the EMI victim. So, the value of Δf is a trade-off between ripple performance and converter EMC.

Let us assume that Δf has been determined by this trade-off: the additional degree of freedom to optimize EMI performance depend on the choice of the modulation. In the triangular modulation, the only parameters left is the modulation index m, that should be large to achieve a flat power spectrum, and small to ensure a fast varying $\xi(t)$. In other words, the choice of m (and or equivalently of the period T assuming Δf fixed) is a second trade-off for maximizing the converter EMC. In a random PAM modulation, in addition to the PAM time symbol T there is an additional degrees of freedom given by the (statistical) properties of the sequence $\{x_k\}$. If we rely on (3) or (4) to fix the symbol (statistical) features [59], and the only parameter left is T, i.e., the modulation index m for the second trade-off to minimize EMI.

[6] A low ripple is not a particularly stringent requirement for LED applications.

The second converter we consider is the resonant class-E converter presented in [87]. This circuit is designed to work with $V_{in} = 5$ V, and to achieve $V_{out} = 12$ V with an output power $P_{out} = 500$ mW when operating with a switching frequency $f_c = 1.25$ MHz and 50% duty cycle. The observed ripple is quite high as in the previous board, measurable in about 300 mV.

As in for the boost converter considered above, Δf is a trade-off between EMC and performance. Here we expect, by increasing Δf, to observe an important reduction also in converter efficiency, since ZVS is not anymore ensured. Furthermore this converter, being a simple proof-of-concept prototype and not a commercial one as in the previous case, has a fixed load and does not embed any output voltage feedback regulation system (usually achieved by means of an on/off control in this kind of converter [88], [114]). For this reason we may expect also a change in the output voltage level due to the introduced modulation.

Also in this case, the choice of the modulation index m is a second trade-off for maximizing the converter EMC.

V. MEASUREMENTS

We provide here some measurements on the two converters introduced in previous section. In order to implement the required spreading function, both converters have been externally driven with an Agilent 33220A arbitrary function generator, programmed to generate a square wave clock modulated in frequency using an externally loaded driving signal. Depending on the measurement, a triangular waveform, the chaotic waveform and the permutation based pseudorandom PAM waveform both proposed in [59] have been loaded into the arbitrary function generator. In the case of the chaotic map the (analog) chaotic waveform has been approximated with a 2048-symbol sequence of 14-bit quantized values.

Emissions from the boards have been measured in the EMI anechoic chamber at the University of Ferrara, by means of an HP85422E spectrum analyzer (certified for EMI measurements). For the sake of simplicity, emissions from the boards have been measured with a HP11941A close-field probe connected to the EMI receiver and placed in proximity of the board inductor, which turned out to be the major source of electromagnetic radiations. This solution guarantees both a simple measurement setup, and reliable results due to the large bandwidth (9 kHz–30 MHz) ensured by the probe and by its calibration. Data for calibration has been loaded into the EMI receiver before measurement session. In all considered cases, the RBW filter bandwidth has been set to the 9 kHz EMI as prescribed to international regulations. An example of the EMI measurement setup is shown in Figure 15.

For output voltage ripple, output voltage level and converter efficiency, measurements have been taken with standard multimeter and digital oscilloscope.

A. CLASS-D CONVERTER

Measurement results on the LM3424 board are shown in Fig. 16, where we plotted, from top to bottom, the peak value of the EMI emitted spectrum, the output voltage ripple (normalized with respect to the unmodulated system ripple) and the efficiency at different values of Δf, of m and with the three different modulation considered.

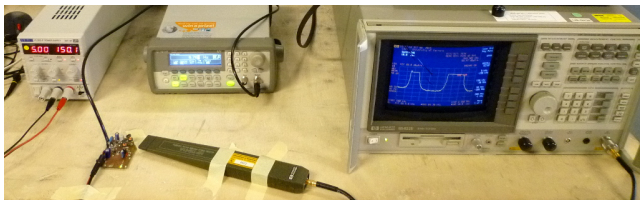

FIGURE 15. Setup for EMI measurements.

Results are aligned with the expected ones. EMI measurements show a minimum for an *intermediate* value of m, which depends on Δf, and ranges in the interval $5 - 20$ for the triangular modulation, and $1 - 5$ for the two PAM based modulations. The higher the Δf, the lower the measured minimum value. Furthermore, while triangular and chaotic modulation have similar performances, the permutation based modulation, as observed in [59], outperforms the other two considered ones by 2–3 dB. The optimum value of m in the plot ensures the highest EMI reduction in measurements when taken accordingly to international regulations. This, of course, does not necessarily correspond to the optimum value for any victim circuit. It is however reasonable assuming that the optimum m value for any victim circuit is not so far from the optimum value shown in Fig. 16.

Ripple measurements show that converter performance is decreasing both with Δf and with m. The main problem we observed is that, when introducing modulation, a low frequency ripple is added as a residual AM of $\xi(t)$. So, the lower $\xi(t)$ frequency (i.e., the higher m), the lower the converter output filter effect, and the higher the ripple. A similar effect can be observed on the converter efficiency, that decreases when Δf or m are increased. This means that the converter performance are optimized by setting both Δf and m as low as possible. Note that this is an additional reason to focus on fast modulations: they not only ensure optimal EMI reduction performance in terms of time domain point of view, but also ensure optimal performance for normal operation of the circuit which is the source of EMI (at least for this switching DC/DC converter).

Top plots of Fig. 16 refer to the first harmonic, where the peak value of the power spectrum is located. It may be interesting to look at the emitted spectrum around the other harmonics. Fig. 17 shows the measured power spectrum for the first 10 harmonics in the triangular modulation case, with $\Delta f = 50$ kHz, and three modulation index values $m = 1$, $m = 5$ and $m = 20$. The value $m = 5$, accordingly to Fig. 16, is that ensuring optimal EMI reduction on the first harmonic for the considered Δf. It may be interesting asking for which values of m we can achieve an optimal EMI reduction around higher order harmonics.

Let us focus on the nth harmonic. Its expression is given by (1) with a Δf that is n times larger but with the same $\xi(t)$,

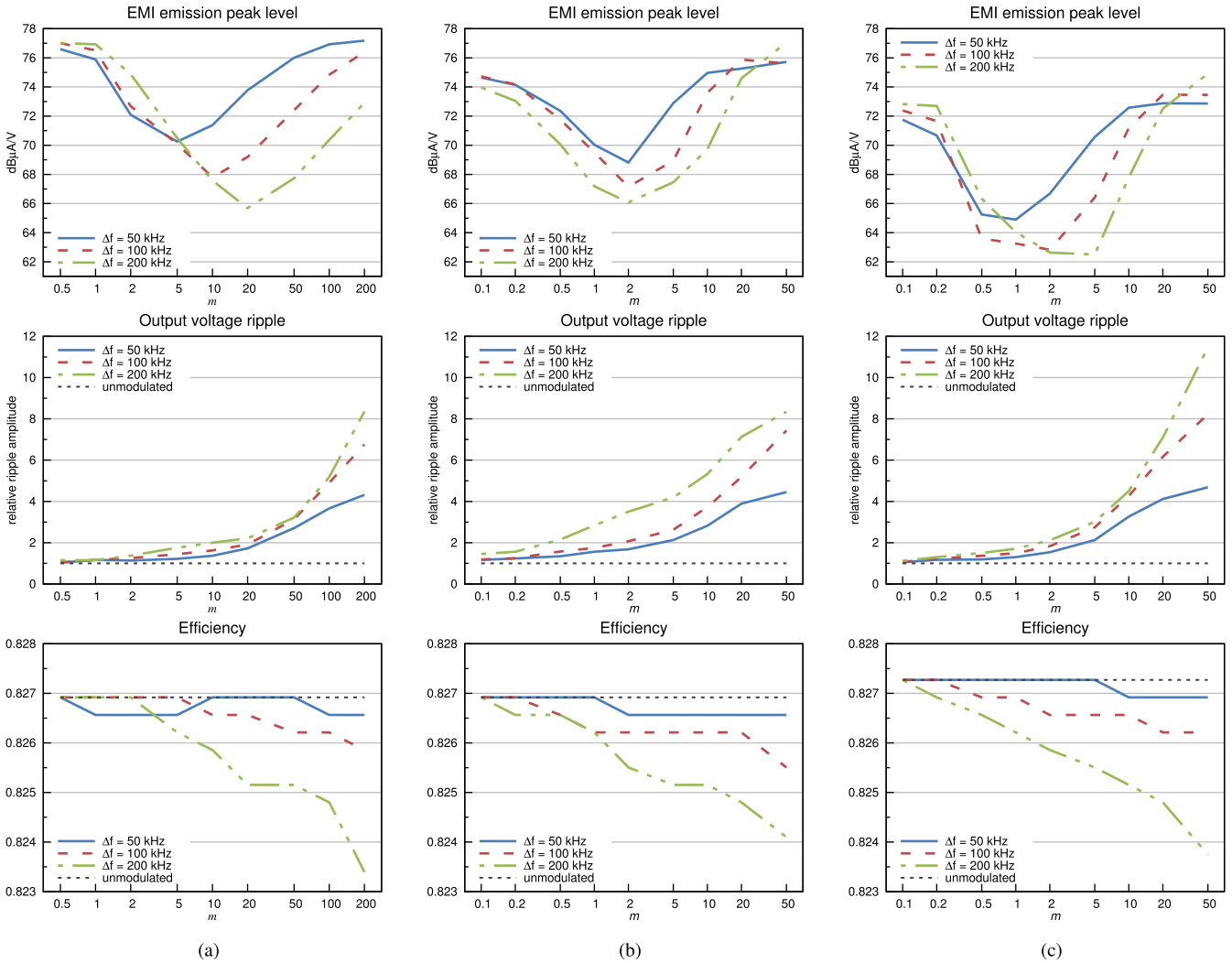

FIGURE 16. Measurements on PWM based boost converter. From top to bottom: EMI emission peak level, relative ripple variation (referred to the unmodulated measured ripple amplitude), efficiency. The considered modulation schemes are: (a): triangular modulation; (b): chaotic PAM modulation; (c): permutation sequence PAM modulation. For the EMI emission measurements, the RBW filter has been set to the 9 kHz EMI filter as accordingly to international regulations for the considered frequency range.

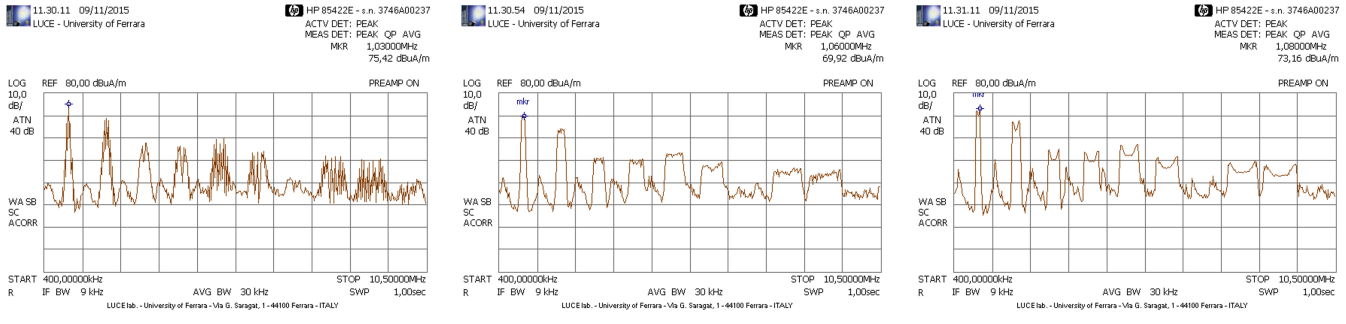

FIGURE 17. Measured power spectra for the PWM based boost converter showing the effect of applying spreading techniques to higher harmonics. A triangular based modulation has been considered, with $f_c = 1$ MHz, $\Delta f = 50$ kHz, and $m = 1$ (a), $m = 5$ (b) and $m = 20$ (c). The RBW filter has been set to the 9 kHz EMI filter as accordingly to international regulations for the considered frequency range.

so when applying results observed on the first harmonic to the nth one we have to consider an *apparent* modulation index m_n that is n times larger with respect to the actual one, i.e., $m_n = n \cdot m$. Furthermore, accordingly to [55] and also to Fig. 16, when Δf increases, the modulation index value required for optimal EMI reduction also increases. Since the

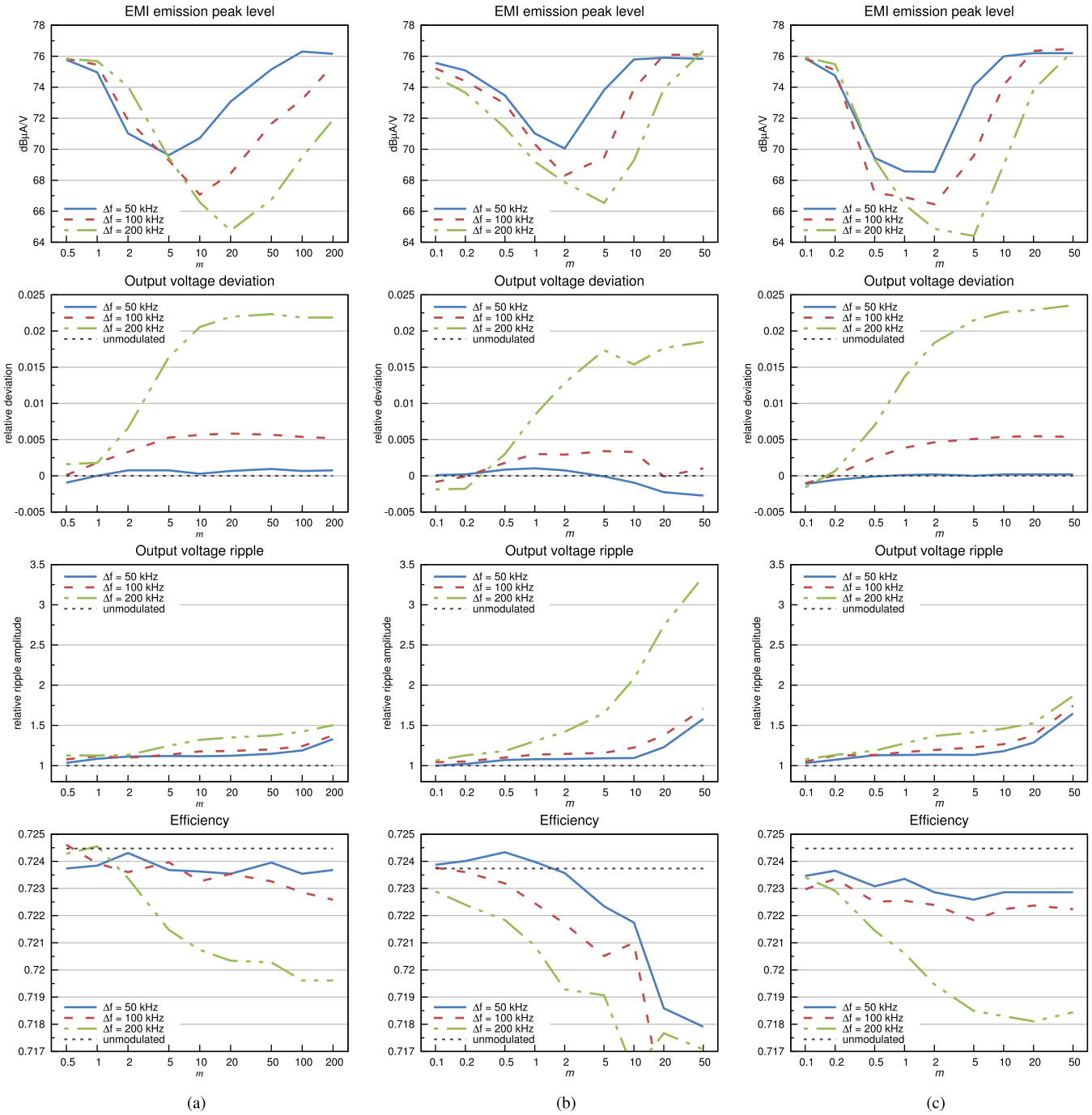

FIGURE 18. Measurements on resonant class-E converter. From top to bottom: EMI emission peak level, relative output voltage deviation, relative ripple variation (referred to the unmodulated measured ripple amplitude), efficiency. The considered modulation schemes are: (a): triangular modulation; (b): chaotic PAM modulation; (c): permutation sequence PAM modulation. For the EMI emission measurements, the RBW filter has been set to the 9 kHz EMI filter as accordingly to international regulations for the considered frequency range.

Carson's bandwidth for the nth harmonic is increasing with n, the optimal value for m_n is then expected to be increasing with n as well. Assuming that the optimal m_n value increases linearly with n, it is easy to conclude that the m value optimizing the nth harmonic is the same optimizing the first one. Despite being far from a precise mathematical demonstration, this suggest that the optimum m value optimizing EMI reduction on the first harmonic may (approximately) optimize *all other harmonics*. By looking at the three spectra of Fig. 17, the value $m = 5$ actually ensure the lowest spectrum values on all harmonics.

B. CLASS-E CONVERTER

Measurement results on the resonant class-E converter are plotted in Fig. 18. From top to bottom, we plotted the peak value of the EMI emitted spectrum, the output

voltage deviation, the output voltage ripple and the efficiency. The output voltage deviation has been measured as the difference from the actual output voltage from the nominal one, and normalized with respect to the nominal output voltage, while the output voltage ripple is normalized with respect to the ripple of the unmodulated case. As for the class D converter, we have considered the three different modulations, three different values of Δf, and several values of m.

EMI measurements confirm the results of the LM3424 evaluation board. The peak in the power spectrum is minimized for an *intermediate* value of m and for large Δf. The permutation based modulation outperforms the other two considered ones by 2–3 dB.

Also measurements on the converter performance confirm the results on LM3424 board. Output voltage ripple and efficiency has the same behavior as in the previous case, while the mean value of the output voltage can be considered unchanged, since a maximum 2% relative variation is observed. As in the previous case, converter performance is optimized using a small Δf and a fast modulation.

VI. CONCLUSION

In this paper, an overview of existing spread spectrum techniques for EMI reduction is provided, considering effects both on the EMI victim and on the circuit implementing the spreading. With the support of measurements on two switching DC/DC converters, we have observed that the spreading depth (i.e. the frequency deviation Δf) need to be determined as a result of a trade-off, since it should be large for EMI reduction and small for reducing performance loss in the converter. More interestingly, also the modulation index m must be the result of a trade-off. To maximize EMI reduction accordingly to the model of the victim circuit, m should have and intermediate value, while it should be as small as possible (i.e., a fast modulation is preferred) in order to minimize ripple and maximize efficiency of the converter emitting the EMI.

REFERENCES

[1] *Code of Federal Regulations 47 (47CFR), Part 15, Subpart B: Unintentional Radiators*. [Online]. Available: http://www.ecfr.gov/, accessed Dec. 1, 2015.

[2] "Council directive on the approximation of the laws of the member states relating to electromagnetic compatibility," Official J. Eur. Union, Tech. Rep. L139/19, May 1989.

[3] M. Li, J. Nuebel, J. L. Drewniak, R. E. DuBroff, T. H. Hubing, and T. P. Van Doren, "EMI from cavity modes of shielding enclosures-FDTD modeling and measurements," *IEEE Trans. Electromagn. Compat.*, vol. 42, no. 1, pp. 29–38, Feb. 2000.

[4] F.-Y. Shih, Y.-T. Chen, Y.-P. Wu, and Y.-T. Chen, "A procedure for designing EMI filters for AC line applications," *IEEE Trans. Power Electron.*, vol. 11, no. 1, pp. 170–181, Jan. 1996.

[5] M. Hartmann, H. Ertl, and J. W. Kolar, "EMI filter design for a 1 MHz, 10 kW three-phase/level PWM rectifier," *IEEE Trans. Power Electron.*, vol. 26, no. 4, pp. 1192–1204, Apr. 2011.

[6] T. Sudo, H. Sasaki, N. Masuda, and J. L. Drewniak, "Electromagnetic interference (EMI) of system-on-package (SOP)," *IEEE Trans. Adv. Packag.*, vol. 27, no. 2, pp. 304–314, May 2004.

[7] S. B. Dhia, M. Ramdani, and E. Sicard, Eds. *Electromagnetic Compatibility of Integrated Circuits: Techniques for low emission and susceptibility*. New York, NY, USA: Springer-Verlag, 2006.

[8] M. Ramdani *et al.*, "The electromagnetic compatibility of integrated circuits—Past, present, and future," *IEEE Trans. Electromagn. Compat.*, vol. 51, no. 1, pp. 78–100, Feb. 2009.

[9] S. Shahparnia and O. M. Ramahi, "Electromagnetic interference (EMI) reduction from printed circuit boards (PCB) using electromagnetic bandgap structures," *IEEE Trans. Electromagn. Compat.*, vol. 46, no. 4, pp. 580–587, Nov. 2004.

[10] E.-P. Li *et al.*, "Progress review of electromagnetic compatibility analysis technologies for packages, printed circuit boards, and novel interconnects," *IEEE Trans. Electromagn. Compat.*, vol. 52, no. 2, pp. 248–265, May 2010.

[11] F. Lin and D. Y. Chen, "Reduction of power supply EMI emission by switching frequency modulation," *IEEE Trans. Power Electron.*, vol. 9, no. 1, pp. 132–137, Jan. 1994.

[12] K. B. Hardin, J. T. Fessler, and D. R. Bush, "Spread spectrum clock generation for the reduction of radiated emissions," in *Proc. IEEE Int. Symp. Electromagn. Compat.*, Aug. 1994, pp. 227–231.

[13] R. Perez, "Power conversion techniques for portable EMI sensitive applications," in *Proc. IEEE Int. Symp. Electromagn. Compat.*, vol. 1. Aug. 2000, pp. 487–491.

[14] E. Zhong and T. A. Lipo, "Improvements in EMC performance of inverter-fed motor drives," *IEEE Trans. Ind. Appl.*, vol. 31, no. 6, pp. 1247–1256, Nov./Dec. 1995.

[15] G. L. Skibinski, R. J. Kerkman, and D. Schlegel, "EMI emissions of modern PWM AC drives," *IEEE Ind. Appl. Mag.*, vol. 5, no. 6, pp. 47–80, Nov./Dec. 1999.

[16] H. Akagi and T. Shimizu, "Attenuation of conducted EMI emissions from an inverter-driven motor," *IEEE Trans. Power Electron.*, vol. 23, no. 1, pp. 282–290, Jan. 2008.

[17] L. Rossetto, S. Buso, and G. Spiazzi, "Conducted EMI issues in a 600-W single-phase boost PFC design," *IEEE Trans. Ind. Appl.*, vol. 36, no. 2, pp. 578–585, Mar./Apr. 2000.

[18] R. Redl, "Electromagnetic environmental impact of power electronics equipment," *Proc. IEEE*, vol. 89, no. 6, pp. 926–938, Jun. 2001.

[19] H. Chung, S. Y. R. Hui, and K. K. Tse, "Reduction of power converter EMI emission using soft-switching technique," *IEEE Trans. Electromagn. Compat.*, vol. 40, no. 3, pp. 282–287, Aug. 1998.

[20] C.-J. Tseng and C.-L. Chen, "A passive lossless snubber cell for non-isolated PWM DC/DC converters," *IEEE Trans. Ind. Electron.*, vol. 45, no. 4, pp. 593–601, Aug. 1998.

[21] K. Fujiwara and H. Nomura, "A novel lossless passive snubber for soft-switching boost-type converters," *IEEE Trans. Power Electron.*, vol. 14, no. 6, pp. 1065–1069, Nov. 1999.

[22] T. Kjellqvist, S. Ostlund, and S. Norrga, "Active snubber circuit for source commutated converters utilizing the IGBT in the linear region," *IEEE Trans. Power Electron.*, vol. 23, no. 5, pp. 2595–2601, Sep. 2008.

[23] D. M. Hockanson, J. L. Drewniak, T. H. Hubing, T. P. Van Doren, F. Sha, and M. J. Wilhelm, "Investigation of fundamental EMI source mechanisms driving common-mode radiation from printed circuit boards with attached cables," *IEEE Trans. Electromagn. Compat.*, vol. 38, no. 4, pp. 557–566, Nov. 1996.

[24] L. Xing and J. Sun, "Conducted common-mode EMI reduction by impedance balancing," *IEEE Trans. Power Electron.*, vol. 27, no. 3, pp. 1084–1089, Mar. 2012.

[25] P. P. Siniscalchi and R. K. Hester, "A 20 W/channel class-D amplifier with near-zero common-mode radiated emissions," *IEEE J. Solid-State Circuits*, vol. 44, no. 12, pp. 3264–3271, Dec. 2009.

[26] M.-L. Yeh, W.-R. Liou, H.-P. Hsieh, and Y.-J. Lin, "An electromagnetic interference (EMI) reduced high-efficiency switching power amplifier," *IEEE Trans. Power Electron.*, vol. 25, no. 3, pp. 710–718, Mar. 2010.

[27] X. Ming, Z. Chen, Z.-K. Zhou, and B. Zhang, "An advanced spread spectrum architecture using pseudorandom modulation to improve EMI in class D amplifier," *IEEE Trans. Power Electron.*, vol. 26, no. 2, pp. 638–646, Feb. 2011.

[28] F. Guanziroli, R. Bassoli, C. Crippa, D. Devecchi, and G. Nicollini, "A 1 W 104 dB SNR filter-less fully-digital open-loop class D audio amplifier with EMI reduction," *IEEE J. Solid-State Circuits*, vol. 47, no. 3, pp. 686–698, Mar. 2012.

[29] H.-H. Chang, I.-H. Hua, and S.-I. Liu, "A spread-spectrum clock generator with triangular modulation," *IEEE J. Solid-State Circuits*, vol. 38, no. 4, pp. 673–676, Apr. 2003.

[30] K. B. Hardin, J. H. Fessler, D. R. Bush, and J. J. Booth, "Spread spectrum clock generator and associated method," U.S. Patent 5 488 627, Jan. 30, 1996.

[31] S. Johnson and R. Zane, "Custom spectral shaping for EMI reduction in high-frequency inverters and ballasts," *IEEE Trans. Power Electron.*, vol. 20, no. 6, pp. 1499–1505, Nov. 2005.
[32] M.-W. Kim, D.-W. Kim, B.-S. Koo, Y.-B. Kim, O.-S. Choi, and N.-D. Kim, "Chip level techniques for EMI reduction in LCD panels," in *Proc. 20th Int. Zurich Symp. Electromagn. Compat.*, Jan. 2009, pp. 441–444.
[33] *Serial ATA Revision 2.6*, Serial ATA Int. Org., Beaverton, OR, USA, Feb. 2007.
[34] M. Aoyama *et al.*, "3 Gbps, 5000 ppm spread spectrum SerDes PHY with frequency tracking phase interpolator for serial ATA," in *Symp. VLSI Circuits Dig. Tech. Papers*, Jun. 2003, pp. 107–110.
[35] M. Kokubo *et al.*, "Spread-spectrum clock generator for serial ATA using fractional PLL controlled by $\Delta\Sigma$ modulator with level shifter," in *IEEE Int. Solid-State Circuits Conf. Dig. Tech. Papers*, Feb. 2005, pp. 160–161 and 590.
[36] H.-R. Lee, O. Kim, G. Ahn, and D.-K. Jeong, "A low-jitter 5000 ppm spread spectrum clock generator for multi-channel SATA transceiver in 0.18 μm CMOS," in *Proc. IEEE Int. Solid-State Circuits Conf.*, Feb. 2005, pp. 162–163 and 590.
[37] D.-S. Shen and S.-L. Liu, "A low-jitter spread spectrum clock generator using FDMP," *IEEE Trans. Circuits Syst. II, Exp. Briefs*, vol. 54, no. 11, pp. 979–983, Nov. 2007.
[38] Y.-H. Kao and Y.-B. Hsieh, "A low-power and high-precision spread spectrum clock generator for serial advanced technology attachment applications using two-point modulation," *IEEE Trans. Electromagn. Compat.*, vol. 51, no. 2, pp. 245–254, May 2009.
[39] F. Pareschi, G. Setti, and R. Rovatti, "A 3-GHz serial ATA spread-spectrum clock generator employing a chaotic PAM modulation," *IEEE Trans. Circuits Syst. I, Reg. Papers*, vol. 57, no. 10, pp. 2577–2587, Oct. 2010.
[40] *VESA DisplayPort Standard Version 1*, Video Electron. Standards Assoc., San Jose, CA, USA, Jan. 2008.
[41] *PCI Express Base Specification1, Revision 1.1*. [Online]. Available: https://pcisig.com/specifications/pciexpress/base, accessed Dec. 1, 2015.
[42] ON Semiconductor. (Nov. 2010). *Low Power, Reduced EMI Clock Synthesizer*. [Online]. Available: http://www.onsemi.com/pub_link/Collateral/NB2780A-D.PDF
[43] *CY25561 Spread Spectrum Clock Generator*, document 38-07242, Cypress Semiconductor Corp., Mar. 2011. [Online]. Available: http://www.cypress.com/?docID=9612
[44] *MB88155 Spread Spectrum Clock Generator*, document DS04-29119-2Ea, Fujitsu Microelectron., Nov. 2006. [Online]. Available: http://www.fujitsu.com/downloads/MICRO/fma/pdf/e429119-2e.pdf
[45] *Multiphase Oscillator With Spread Spectrum Frequency Modulation*, document LTC6902, Linear Technology, 2003. [Online]. Available: http://cds.linear.com/docs/en/datasheet/6902f.pdf
[46] K. K. Tse, H. S.-H. Chung, S. Y. Huo, and H. C. So, "Analysis and spectral characteristics of a spread-spectrum technique for conducted EMI suppression," *IEEE Trans. Power Electron.*, vol. 15, no. 2, pp. 399–410, Mar. 2000.
[47] K. K. Tse, H. S.-H. Chung, S. Y. R. Hui, and H. C. So, "A comparative study of carrier-frequency modulation techniques for conducted EMI suppression in PWM converters," *IEEE Trans. Ind. Electron.*, vol. 49, no. 3, pp. 618–627, Jun. 2002.
[48] J. Balcells, A. Santolaria, A. Orlandi, D. Gonzalez, and J. Gago, "EMI Reduction in Switched Power Converters using Frequency Modulation Techniques," *IEEE Trans. Electromagn. Compat.*, vol. 47, no. 3, pp. 569–576, Aug. 2005.
[49] D. Gonzalez *et al.*, "Conducted EMI reduction in power converters by means of periodic switching frequency modulation," *IEEE Trans. Power Electron.*, vol. 22, no. 6, pp. 2271–2281, Nov. 2007.
[50] K. K. Tse, R. W.-M. Ng, H. S.-H. Chung, and S. Y. R. Hui, "An evaluation of the spectral characteristics of switching converters with chaotic carrier-frequency modulation," *IEEE Trans. Ind. Electron.*, vol. 50, no. 1, pp. 171–182, Feb. 2003.
[51] A. M. Stankovic, G. C. Verghese, and D. J. Perreault, "Analysis and synthesis of randomized modulation schemes for power converters," *IEEE Trans. Power Electron.*, vol. 10, no. 6, pp. 680–693, Nov. 1995.
[52] A. M. Stanković and H. Lev-Hari, "Randomized modulation in power electronic converters," *Proc. IEEE*, vol. 90, no. 5, pp. 782–799, May 2002.
[53] "LM5088 evaluation board," Texas Instrum., Dallas, TX, USA, Appl. Note 1913. [Online]. Available: http://www.ti.com/lit/ug/snva379e/snva379e.pdf, accessed Dec. 1, 2015.
[54] ON Semiconductor. (2010). *P6P82PS01A: A 'Drop-In' Active EMI Reduction IC For AC-DC and DC-DC Power Converters*. [Online]. Available: http://www.onsemi.com/pub_link/Collateral/AND8477-D.PDF
[55] F. Pareschi, G. Setti, R. Rovatti, and G. Frattini, "Practical optimization of EMI reduction in spread spectrum clock generators with application to switching DC/DC converters," *IEEE Trans. Power Electron.*, vol. 29, no. 9, pp. 4646–4657, Sep. 2014.
[56] S. Callegari, R. Rovatti, and G. Setti, "Spectral properties of chaos-based FM signals: Theory and simulation results," *IEEE Trans. Circuits Syst. I, Fundam. Theory Appl.*, vol. 50, no. 1, pp. 3–15, Jan. 2003.
[57] Y. Matsumoto, K. Fujii, and A. Sugiura, "An analytical method for determining the optimal modulating waveform for dithered clock generation," *IEEE Trans. Electromagn. Compat.*, vol. 47, no. 3, pp. 577–584, Aug. 2005.
[58] D. De Caro, "Optimal discontinuous frequency modulation for spread-spectrum clocking," *IEEE Trans. Electromagn. Compat.*, vol. 55, no. 5, pp. 891–900, Oct. 2013.
[59] F. Pareschi, G. Setti, R. Rovatti, and G. Frattini, "Short-term optimized spread spectrum clock generator for EMI reduction in switching DC/DC converters," *IEEE Trans. Circuits Syst. I, Reg. Papers*, vol. 61, no. 10, pp. 3044–3053, Oct. 2014.
[60] *FCC Methods of Measurement of Radio Noise Emission From Computing Devices*, document FCC/OST MP-4, Federal Communication Commission, Jul. 1987.
[61] *Specification for Radio Disturbance and Immunity Measuring Apparatus and Methods—Part 1-1: Radio Disturbance and Immunity Measuring Apparatus—Measuring Apparatus*, document CISPR 16-1-1, International Special Committee on Radio Interference, 2010.
[62] *Specification for Radio Disturbance and Immunity Measuring Apparatus and Methods—Part 2-1: Methods of Measurement of Disturbances and Immunity—Conducted Disturbance Measurements*, document CISPR 16-2-1, International Special Committee on Radio Interference, 2010.
[63] A. Santolaria, "Effects of switching frequency modulation on the power converter's output voltage," *IEEE Trans. Ind. Electron.*, vol. 56, no. 7, pp. 2729–2737, Jul. 2009.
[64] H. S. Black, *Modulation Theory*. New York, NY, USA: Van Nostrand, 1953.
[65] J. D. Gibson, Eds., *Mobile Communications Handbook*. Piscataway, NJ, USA: IEEE Press, 1996.
[66] D. De Caro, C. A. Romani, N. Petra, A. G. M. Strollo, and C. Parrella, "A 1.27 GHz, all-digital spread spectrum clock generator/synthesizer in 65 nm CMOS," *IEEE J. Solid-State Circuits*, vol. 45, no. 5, pp. 1048–1060, May 2010.
[67] S.-W. Oh, H.-M. Park, J.-H. Seo, J.-Y. Jang, G.-Y. Bae, and J.-K. Kang, "A 60 to 200 MHz SSCG with approximate Hershey-Kiss modulation profile in 0.11 μm CMOS," in *Proc. Int. SoC Design Conf. (ISOCC)*, Nov. 2012, pp. 423–426.
[68] M. Song, S. Ahn, I. Jung, Y. Kim, and C. Kim, "Piecewise linear modulation technique for spread spectrum clock generation," *IEEE Trans. Very Large Scale Integr. (VLSI) Syst.*, vol. 21, no. 7, pp. 1234–1245, Jul. 2013.
[69] R. Saraswat, U. Zillmann, S. Supriyanto, G. Droege, and U. Bretthauer, "Programmable spread spectrum clock generation based on successive phase selection technique," in *Proc. IEEE Int. Symp. Circuits Syst. (ISCAS)*, May 2008, pp. 2845–2848.
[70] G. Setti, M. Balestra, and R. Rovatti, "Experimental verification of enhanced electromagnetic compatibility in chaotic FM clock signals," in *Proc. IEEE Int. Symp. Circuits Syst.*, vol. 3. May 2000, pp. 229–232.
[71] A. J. Menezes, P. C. van Oorschot, and S. A. Vanstone, *Handbook of Applied Cryptography*. Boca Raton, FL, USA: CRC Press, 1996.
[72] P. L'Ecuyer and R. Simard, "TestU01: A C library for empirical testing of random number generators," *AMC Trans. Math. Softw.*, vol. 33, no. 4, Aug. 2007, Art. ID 22.
[73] F. Pareschi, R. Rovatti, and G. Setti, "On statistical tests for randomness included in the NIST SP800-22 test suite and based on the binomial distribution," *IEEE Trans. Inf. Forensics Security*, vol. 7, no. 2, pp. 491–505, Apr. 2012.
[74] A. Lasota and M. Mackey, *Chaos, Fractals, and Noise: Stochastic Aspects of Dynamics* (Applied Mathematical Sciences), vol. 97, 2nd ed. Cambridge, U.K.: Cambridge Univ. Press, 1994.

[75] G. Setti, G. Mazzini, R. Rovatti, and S. Callegari, "Statistical modeling of discrete-time chaotic processes-basic finite-dimensional tools and applications," *Proc. IEEE*, vol. 90, no. 5, pp. 662–690, May 2002.
[76] R. Rovatti, G. Mazzini, G. Setti, and A. Giovanardi, "Statistical modeling and design of discrete-time chaotic processes: Advanced finite-dimensional tools and applications," *Proc. IEEE*, vol. 90, no. 5, pp. 820–841, May 2002.
[77] T. Regan and D. La Porte, "Easy-to-use spread spectrum clock generator reduces EMI and more," Linear Technol. Mag., pp. 9–12. [Online]. Available: http://cds.linear.com/docs/en/lt-journal/LT6902_0204_Mag.pdf, accessed Dec. 1, 2015.
[78] N. Da Dalt, P. Pridnig, and W. Grollitsch, "An all-digital PLL using random modulation for SSC generation in 65 nm CMOS," in *IEEE Int. Solid-State Circuits Conf. Dig. Tech. Papers (ISSCC)*, Feb. 2013, pp. 252–253.
[79] L. A. De Michele, F. Pareschi, R. Rovatti, and G. Setti, "Chaos-based high-EMC spread-spectrum clock generator," in *Proc. Eur. Conf. Circuit Theory Design (ECCTD)*, vol. 1. Aug. 2005, pp. I-165–I-168.
[80] A. Wang and S. R. Sanders, "Random and programmed pulse-width modulation techniques for DC-DC converters," in *Proc. IEEE Int. Conf. Syst. Eng.*, Aug. 1990, pp. 589–592.
[81] F. Mihalic and D. Kos, "Reduced conductive EMI in switched-mode DC–DC power converters without EMI filters: PWM versus randomized PWM," *IEEE Trans. Power Electron.*, vol. 21, no. 6, pp. 1783–1794, Nov. 2006.
[82] T. Tanaka, T. Ninomiya, and K. Harada, "Random-switching control in DC-to-DC converters," in *Proc. Rec. 20th Annu. IEEE Power Electron. Specialists Conf. (PESC)*, vol. 1. Jun. 1989, pp. 500–507.
[83] C. K. Tse and M. di Bernardo, "Complex behavior in switching power converters," *Proc. IEEE*, vol. 90, no. 5, pp. 768–781, May 2002.
[84] A. Knott, G. Pfaffinger, and M. A. E. Andersen, "Comparison of three different modulators for power converters with respect to EMI optimization," in *Proc. IEEE Int. Symp. Ind. Electron. (ISIE)*, Jun./Jul. 2008, pp. 117–123.
[85] R. Ramamurthy and P. V. Ranjan, "Modeling and simulation of psm buck converter under dcm," *Eur. J. Sci. Res.*, vol. 47, no. 2, pp. 241–247, 2010.
[86] J. Sun, "Pulse-width modulation," in *Dynamics and Control of Switched Electronic Systems*, F. Vasca and L. Iannelli, Eds. London, U.K.: Springer-Verlag, 2012, ch. 2, pp. 25–61.
[87] N. Bertoni, G. Frattini, R. Massolini, F. Pareschi, R. Rovatti, and G. Setti, "A new semi-analytic approach for class-E resonant DC-DC converter design," *IEEE Trans. Power Electron.*, to appear, 2016.
[88] R. C. N. Pilawa-Podgurski, A. D. Sagneri, J. M. Rivas, D. I. Anderson, and D. J. Perreault, "Very high frequency resonant boost converters," *IEEE Trans. Power Electron.*, vol. 24, no. 6, pp. 1654–1665, Jun. 2009.
[89] F. Pareschi, T. Vincenzi, M. Mangia, N. Bertoni, R. R. Rovatti, and G. Setti, "Application of spread-spectrum techniques to class-E DC/DC converters: Some preliminary results," in *Proc. IEEE Nordic Conf. Circuits Syst. (NORCAS)*, Oct. 2015.
[90] L. A. Barragan, D. Navarro, J. Acero, I. Urriza, and J. M. Burdío, "FPGA implementation of a switching frequency modulation circuit for EMI reduction in resonant inverters for induction heating appliances," *IEEE Trans. Ind. Electron.*, vol. 55, no. 1, pp. 11–20, Jan. 2008.
[91] F. Fiori, "Design of an operational amplifier input stage immune to EMI," *IEEE Trans. Electromagn. Compat.*, vol. 49, no. 4, pp. 834–839, Nov. 2007.
[92] J. Yu, A. Amer, and E. Sanchez-Sinencio, "Electromagnetic interference resisting operational amplifier," *IEEE Trans. Circuits Syst. I, Reg. Papers*, vol. 61, no. 7, pp. 1917–1927, Jul. 2014.
[93] E. Orietti, N. Montemezzo, S. Buso, G. Meneghesso, A. Neviani, and G. Spiazzi, "Reducing the EMI susceptibility of a Kuijk bandgap," *IEEE Trans. Electromagn. Compat.*, vol. 50, no. 4, pp. 876–886, Nov. 2008.
[94] J. Laurin, S. G. Zaky, and K. G. Balmain, "EMI-induced failures in crystal oscillators," *IEEE Trans. Electromagn. Compat.*, vol. 33, no. 4, pp. 334–342, Nov. 1991.
[95] J. Laurin, S. G. Zaky, and K. G. Balmain, "On the prediction of digital circuit susceptibility to radiated EMI," *IEEE Trans. Electromagn. Compat.*, vol. 37, no. 4, pp. 528–535, Nov. 1995.
[96] R. Hoad, N. J. Carter, D. Herke, and S. P. Watkins, "Trends in EM susceptibility of IT equipment," *IEEE Trans. Electromagn. Compat.*, vol. 46, no. 3, pp. 390–395, Aug. 2004.
[97] L. B. Gravelle and P. F. Wilson, "EMI/EMC in printed circuit boards—A literature review," *IEEE Trans. Electromagn. Compat.*, vol. 34, no. 2, pp. 109–116, May 1992.
[98] M. G. Backstrom and K. G. Lovstrand, "Susceptibility of electronic systems to high-power microwaves: Summary of test experience," *IEEE Trans. Electromagn. Compat.*, vol. 46, no. 3, pp. 396–403, Aug. 2004.
[99] K. B. Hardin, J. T. Fessler, and D. R. Bush, "A study of the interference potential of spread spectrum clock generation techniques," in *Proc. IEEE Int. Symp. Electromagn. Compat.*, Aug. 1995, pp. 624–629.
[100] H. G. Skinner and K. P. Slattery, "Why spread spectrum clocking of computing devices is not cheating," in *Proc. IEEE Int. Symp. Electromagn. Compat.*, vol. 1. Aug. 2001, pp. 537–540.
[101] K. Hardin, R. A. Oglesbee, and F. Fisher, "Investigation into the interference potential of spread-spectrum clock generation to broadband digital communications," *IEEE Trans. Electromagn. Compat.*, vol. 45, no. 1, pp. 10–21, Feb. 2003.
[102] I. Gil and R. Fernandez-Garcia, "Characterization and modelling of emi susceptibility in integrated circuits at high frequency," in *Proc. Int. Symp. Electromagn. Compat. (EMC EUROPE)*, Sep. 2012, pp. 1–6.
[103] "Understanding dynamic signal analysis," Agilent Technol., Santa Clara, CA, USA, Appl. Note 1405-2. [Online]. Available: http://www.testunlimited.com/pdf/an/5988-6774EN.pdf, accessed Dec. 1, 2015.
[104] "Spectrum analysis basics," Agilent Technol., Santa Clara, CA, USA, Appl. Note 150. [Online]. Available: http://cp.literature.agilent.com/litweb/pdf/5952-0292.pdf, accessed Dec. 1, 2015.
[105] J. G. Proakis, *Digital Communications*, 4th ed. New York, NY, USA: McGraw-Hill, Aug. 2000.
[106] *Information Technology equipment—Radio Disturbance Characteristics—Limits and Methods of Measurement*, document 22-5-2, International Special Committee on Radio Interference, 2006.
[107] "Making EMI compliance measurements," Keysight, Santa Rosa, CA, USA, Appl. Note. [Online]. Available: http://literature.cdn.keysight.com/litweb/pdf/5990-7420EN.pdf, accessed Dec. 1, 2015.
[108] S. Braun, A. Frech, and P. Russer, "CISPR specification and measurement uncertainty of the time-domain EMI measurement system," in *Proc. IEEE Int. Symp. Electromagn. Compat. (EMC)*, Aug. 2008, pp. 1–4.
[109] M. Keller and K.-H. Weidner, "The world's fastest EMI test receiver drastically reduces testing times," Rohde & Schwarz, Munich, Germany, Tech. Rep. 207, 2012.
[110] F. Krug and P. Russer, "Quasi-peak detector model for a time-domain measurement system," *IEEE Trans. Electromagn. Compat.*, vol. 47, no. 2, pp. 320–326, May 2005.
[111] T. Karaca, B. Deutschmann, and G. Winkler, "EMI-receiver simulation model with quasi-peak detector," in *Proc. IEEE Int. Symp. Electromagn. Compat. (EMC)*, Aug. 2015, pp. 891–896.
[112] F. Pareschi and G. Setti. *MATLAB Simulator of an EMI Receiver*. [Online]. Available: www.signalprocessing.it, accessed Dec. 1, 2015.
[113] "LM3424 buck-boost evaluation board," Texas Instrum., Dallas, TX, USA, Appl. Note 1967. [Online]. Available: http://www.ti.com/lit/ug/snva397a/snva397a.pdf, accessed Dec. 1, 2015.
[114] Y. S. Lee and Y. C. Cheng, "A 580 kHz switching regulator using on-off control," *J. Inst. Electron. Radio Eng.*, vol. 57, no. 5, pp. 221–226, Sep. 1987.

FABIO PARESCHI (S'05–M'08) received the D.Eng. (Hons.) degree in electronics engineering from the University of Ferrara, Italy, in 2001, and the Ph.D. degree in information technology under the European Doctorate Project from the University of Bologna, Italy, in 2007. In 2006, he spent six months as a Visiting Scholar with the Department of Electrical Engineering, Catholic University of Leuven, Belgium. He is currently an Assistant Professor with the Department of Engineering, University of Ferrara. He is also a Faculty Member with the Advanced Research Center on Electronic Systems, University of Bologna. He served as an Associate Editor of the IEEE TRANSACTIONS ON CIRCUITS AND SYSTEMS—PART II (2010-2013). He was a co-recipient of the best paper award at ECCTD 2005 and the Best Student Paper Award at EMC Zurich 2005.

RICCARDO ROVATTI (M'99–SM'02–F'12) received the M.S. degree in electronics engineering and the Ph.D. degree in electronics, computer science, and telecommunications from the University of Bologna, Italy, in 1992 and 1996, respectively. He has authored approximately 300 technical contributions to international conferences and journals, and two volumes. His research focuses on mathematical and applicative aspects of statistical signal processing and on the application of statistics to nonlinear dynamical systems. He received the 2004 IEEE CAS Society Darlington Award, the 2013 IEEE CAS Society Guillemin-Cauer Award, the best paper award at ECCTD 2005, and the Best Student Paper Award at EMC Zurich 2005 and ISCAS 2011.

GIANLUCA SETTI (S'89–M'91–SM'02–F'06) received the Ph.D. degree in electronic engineering and computer science from the University of Bologna, in 1997. Since 1997, he has been with the School of Engineering, University of Ferrara, Italy, where he is currently a Professor of Circuit Theory and Analog Electronics and a Permanent Faculty Member with ARCES–University of Bologna, Italy. His research interests include nonlinear circuits, implementation and application of chaotic circuits and systems, electromagnetic compatibility, statistical signal processing, and biomedical circuits and systems. He received the 2013 IEEE CAS Society Meritorious Service Award and was a co-recipient of the 2004 IEEE CAS Society Darlington Award, the 2013 IEEE CAS Society Guillemin-Cauer Award, the best paper award at ECCTD 2005, and the Best Student Paper Award at EMC Zurich 2005 and at ISCAS 2011. He held several editorial positions and served, in particular, as the Editor-in-Chief of the IEEE TRANSACTIONS ON CIRCUITS AND SYSTEMS PART II (2006-2007) and the IEEE RANSACTIONS ON CIRCUITS AND SYSTEMS PART I (2008-2009). He was the Technical Program Co-Chair of ISCAS 2007 and 2008, ICECS 2012, and BioCAS 2013, and the General Co-Chair of NOLTA 2006. He was a member of the Board of Governors of the IEEE CAS Society (2005-2008), served as its 2010 President, and is a Distinguished Lecturer of CASS (2015-2016). He held several other volunteer positions for the IEEE and was the first Non North-American Vice President of the IEEE for Publication Services and Products from 2013 to 2014.